Siglec-H protects from virus-triggered severe systemic autoimmunity

Heike Schmitt,[1] Sabrina Sell,[2] Julia Koch,[1] Martina Seefried,[2] Sophia Sonnewald,[3] Christoph Daniel,[4] Thomas H. Winkler,[2]* and Lars Nitschke[1]*

[1]Division of Genetics, Department of Biology, [2]Nikolaus-Fiebiger-Zentrum, Division of Genetics, Department of Biology, [3]Division of Biochemistry, Department of Biology, and [4]Department of Nephropathology, University of Erlangen-Nürnberg, 91054 Erlangen, Germany

It is controversial whether virus infections can contribute to the development of autoimmune diseases. Type I interferons (IFNs) are critical antiviral cytokines during virus infections and have also been implicated in the pathogenesis of systemic lupus erythematosus. Type I IFN is mainly produced by plasmacytoid dendritic cells (pDCs). The secretion of type I IFN of pDCs is modulated by Siglec-H, a DAP12-associated receptor on pDCs. In this study, we show that Siglec-H–deficient pDCs produce more of the type I IFN, IFN-α, in vitro and that Siglec-H knockout (KO) mice produce more IFN-α after murine cytomegalovirus (mCMV) infection in vivo. This did not impact control of viral replication. Remarkably, several weeks after a single mCMV infection, Siglec-H KO mice developed a severe form of systemic lupus–like autoimmune disease with strong kidney nephritis. In contrast, uninfected aging Siglec-H KO mice developed a mild form of systemic autoimmunity. The induction of systemic autoimmune disease after virus infection in Siglec-H KO mice was accompanied by a type I IFN signature and fully dependent on type I IFN signaling. These results show that Siglec-H normally serves as a modulator of type I IFN responses after infection with a persistent virus and thereby prevents induction of autoimmune disease.

The Journal of Experimental Medicine

Systemic lupus erythematosus (SLE) is a chronic autoimmune inflammatory disorder with a complex multifactorial pathogenesis. This systemic autoimmune disease is characterized by the production of autoantibodies, immune complex deposition leading to tissue injury, and kidney nephritis (Jacobi and Diamond, 2005; Rahman and Isenberg, 2008). Besides gender bias with a higher prevalence in women, SLE has a high heritability, and complex multigenetic factors have an impact on the susceptibility of the disease. Different genome-wide association studies revealed at least 25 loci that have been associated with susceptibility to SLE. Most of these loci affect genes that are involved in immune complex processing, TLR function, and type I IFN production as well as in lymphocyte signaling (Cervino et al., 2007; Harley et al., 2009; Moser et al., 2009). IFNs have been linked to SLE pathophysiology since the 1970s (Hooks et al., 1979). Further studies revealed a correlation between aberrant increased expression of IFN-α and human SLE (Preble et al., 1982) as well as an IFN signature in most patients with active SLE (Baechler et al., 2003; Bennett et al., 2003).

Autoantibodies in SLE are often directed against DNA, RNA, or nuclear complexes containing nucleic acids. There is good evidence that TLRs like TLR7 or TLR9, which are pattern recognition receptors and bind single-stranded RNA or DNA, respectively, can be activated not only by bacterial or viral nucleic acids, but also by endogenous ligands in the form of immune complexes (Marshak-Rothstein, 2006; Marshak-Rothstein and Rifkin, 2007). The activation of TLR7 and TLR9 by immune complexes containing self-proteins and nucleic acids leads to the production of type I IFN. These immune complexes containing nucleic acids may originate from dying cells. Defective clearance of dying cells has been observed in SLE (Baumann et al., 2002). Furthermore, intracellular cytoplasmic sensors of DNA and RNA, such as stimulator of type I IFN genes, are also involved in type I IFN production (Sharma et al., 2015). The innate immune cells that generate most type I IFNs are plasmacytoid DCs (pDCs). pDCs develop in the BM and can secrete rapidly large amounts of type I IFNs, i.e., IFN-α or IFN-β, upon stimulation of their endosomal TLR7 and TLR9 or cytoplasmic nucleic acid sensors (Colonna et al., 2004; Liu, 2005).

In both mice and humans, an efficient host defense against virus depends on a robust IFN-α response, especially early during virus infections (Zucchini et al., 2008; Swiecki et al., 2010). As pDCs constitutively express TLR9, virus DNA of DNA viruses such as CMV can bind to TLR9 and trigger type I IFN production by these cells (Krug et al., 2004). pDCs are critical for induction of early high type I IFN levels after virus infection. However, pDC depletion experiments and genetic mouse models showed that pDCs and TLR signaling

*T.H. Winkler and L. Nitschke contributed equally to this paper.

Correspondence to Lars Nitschke: lars.nitschke@fau.de; or Thomas H. Winkler: thomas.winkler@fau.de

Abbreviations used: ANA, antinuclear antibody; BUN, blood urea nitrogen; dsDNA, double-stranded DNA; IFNAR, IFN-α/β receptor; mCMV, murine CMV; nRNP, nuclear ribonucleoprotein; pDC, plasmacytoid DC; p.i., peritoneal injection; qRT-PCR, quantitative RT-PCR; SLE, systemic lupus erythematosus.

The Rockefeller University Press $30.00
J. Exp. Med. 2016 Vol. 213 No. 8 1627–1644
www.jem.org/cgi/doi/10.1084/jem.20160189

are dispensable for type I IFN responses during a CMV infection (Swiecki et al., 2010; Cocita et al., 2015). These experiments suggest that other cell types than pDCs contribute to type I IFN production during viral infections. Similarly, type I IFN responses in humans are crucial for antiviral defense, but TLR signaling is not required (von Bernuth et al., 2012).

Because most SLE patients show a type I IFN signature, it is a controversial matter whether release of type I IFN after a virus infection may be involved in triggering this autoimmune disease. Acute viral infections such as EBV or hepatitis B virus can induce transient production of autoantibodies (McFarlane et al., 1995; Hansen et al., 1998; Harley and James, 2006), but it is unclear whether they can induce a systemic autoimmune disease. The mechanisms discussed for this transient autoantibody production after viral infection are uncontrolled cellular release of type I IFN or molecular mimicry of viral antigens with autoantigens (Bogdanos et al., 2000; Sundar et al., 2004; Harley and James, 2006).

Sialic acid–binding Ig-type lectin H (Siglec-H) is expressed on mouse pDCs and is a commonly used pDC marker (Blasius et al., 2006; Zhang et al., 2006). Siglec-H is also expressed on a subset of DC precursors in the BM (Schlitzer et al., 2015), a subset of marginal zone macrophages in the spleen, medullary macrophages in lymph nodes (Zhang et al., 2004), and microglia in the brain (Kopatz et al., 2013). Although many Siglec receptors have immunoreceptor tyrosine-based inhibition motifs, Siglec-H lacks such a motif but is associated with DAP12, which is necessary for its surface expression on pDCs (Blasius et al., 2006). It was shown that antibody-mediated cross-linking of Siglec-H reduces type I IFN production by pDCs in response to CpG administration in vitro and in vivo (Blasius et al., 2004). Furthermore, Siglec-H–deficient pDCs produce elevated levels of IFN-α after TLR ligand stimulation in vitro (Takagi et al., 2011). This was not confirmed by another study (Swiecki et al., 2014). It was also shown that Siglec-H–deficient mice produce more IFN-α after murine CMV (mCMV) infection in vivo (Puttur et al., 2013). Here, we examined whether Siglec-H deficiency has an influence on viral clearance after mCMV infection and whether this deficiency leads to development of autoimmunity. We show that Siglec-H is responsible for controlling the type I IFN response after mCMV infection and for preventing the virus-induced development of systemic autoimmune disease.

RESULTS

Siglec-H deficiency leads to increased IFN-α production after TLR stimulation of pDCs in vitro and during the acute phase of mCMV infection in vivo

The Siglec-H KO mouse line used in this study was obtained from the Consortium for Functional Glycomics (Orr et al., 2013). Because this mouse line has not been characterized in detail, we confirmed via flow cytometry that pDCs from Siglec-H KO mice do not express Siglec-H on their surface (Fig. S1 A). Furthermore, the absence of Siglec-H does not alter the numbers of pDCs in different organs (Fig. S1 B). As controversial results about IFN-α secretion after CpG or mCMV stimulation of Siglec-H$^{-/-}$ pDCs have been published (Takagi et al., 2011; Swiecki et al., 2014), we analyzed pDC stimulation in our independently generated Siglec-H–deficient mouse line. In vitro–generated pDCs of Siglec-H KO mice secreted increased IFN-α levels after stimulation with CpG-A, whereas IFN-γ was similarly induced in Siglec-H and WT mice (Fig. 1 A). Similarly, when pDCs were stimulated with mCMV in vitro, enhanced IFN-α secretion was detected (Fig. 1 B). When Siglec-H KO mice were infected with mCMV, we observed that Siglec-H KO mice produce significantly higher amounts of IFN-α on day 1 and day 2 of peritoneal injection (p.i.) but not increased levels of IFN-γ (Fig. 1 C). Serum levels of IFN-α normalized 7 d after infection in both WT and Siglec-H KO mice.

mCMV-infected Siglec-H KO mice control virus replication similarly to WT animals

As type I IFN is crucial for virus defense, we infected Siglec-H KO and WT control mice with 5×10^5 PFU of a Smith strain of mCMV encoding luciferase and lacking the m157 gene (MCMV157luc) and measured viral load by a luciferase assay in samples of different organs. Siglec-H KO mice showed a slight reduction of viral load in liver and lung at 2 d after p.i. with mCMV, but not in other organs, when compared with WT mice. Overall control of viral load was similar at the later time points day 5 and day 7 (Fig. 2 A). $CD8^+$ T cells (together with NK cells) are the most important effector cells for mCMV control. Thus, we examined the intracellular IFN-γ production by mCMV-specific $CD8^+$ T cells after restimulation with a mixture of mCMV-specific peptides M33, M45, and M139 7 d and 10 wk after p.i. Our data indicate that the absence of Siglec-H does not alter the number of mCMV-specific T cells generated in response to infection (Fig. 2 B). Virus infection of Siglec-H KO mice may also affect localization or numbers of pDCs. Hence, we analyzed pDC numbers at 1, 10, and 26 wk after p.i. with mCMV in different organs of WT and Siglec-H KO mice and could not detect any differences (unpublished data).

Aging Siglec-H KO mice develop mild signs of an autoimmune disease

To address the question of whether Siglec-H deficiency can lead to a spontaneous systemic autoimmunity caused by higher levels of IFN-α, we analyzed aging WT and Siglec-H KO mice for typical signs of autoimmunity. Indeed, 60-wk-old Siglec-H KO mice showed a significant increase of anti–double-stranded DNA (dsDNA) IgG antibodies (Fig. 3 A), antinuclear antibodies (ANAs; Fig. 3 B), and proteinuria (Fig. 3 C). However, we could not detect severe changes in kidney histology (unpublished data). The autoimmune phenotype was observed in 60-wk-old mice but absent in 12- and 36-wk-old mice (unpublished data). Our results indicate that the absence of Siglec-H triggers the development of a mild lupus-like disease in aging Siglec-H KO mice.

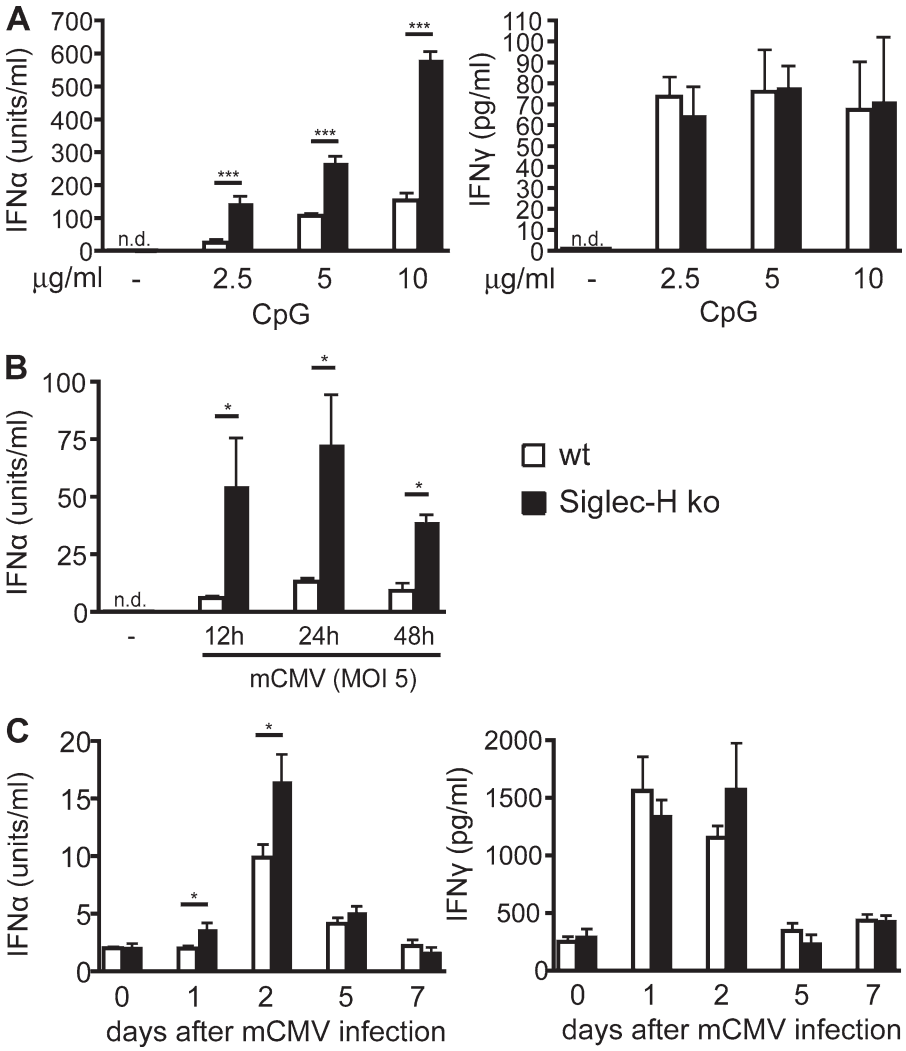

Figure 1. **IFN-α levels are elevated in the absence of Siglec-H upon CpG stimulation in vitro and mCMV infection in vivo.** (A) BM-derived and sorted PDCA$^+$CD11c$^+$ pDCs from WT (wt) and Siglec-H KO (ko) mice were stimulated for 48 h with increasing concentrations of CpG-A. IFN-α and IFN-γ levels in the supernatants were detected by ELISA. Data are combined from three independent experiments (n = 9). (B) BM-derived and sorted PDCA$^+$CD11c$^+$ pDCs from WT and Siglec-H KO mice were stimulated for 12, 24, and 48 h with luciferase-encoding mCMV (MCMV157luc). IFN-α was detected by ELISA (n = 5). Data are representative of three independent experiments. MOI, multiplicity of infection. (C) WT and Siglec-H KO mice were infected with 5×10^5 PFU MCMV157luc, and the kinetics of serum IFN-α and IFN-γ evels 0, 1, 2, 5, and 7 d after infection was measured via ELISA. Data are representative of three independent experiments (n = 6 for each experiment). *, $P < 0.05$; ***, $P < 0.001$; Student's t test (A) and Mann-Whitney (B and C) test. Bar graphs show mean values with SEM. n.d., not detectable.

mCMV infection causes a severe lupus-like phenotype in Siglec-H KO mice

Viral infections have been shown to induce a transient generation of autoantibodies (McFarlane et al., 1995; Hansen et al., 1998; Harley and James, 2006). As we observed higher levels of IFN-α in vitro and in vivo and signs of autoimmunity in aging Siglec-H KO mice, we next wanted to investigate whether a virus infection of Siglec-H KO mice can trigger systemic autoimmunity. To this end, we infected WT and Siglec-H KO mice once with 5×10^5 PFU mCMV and monitored typical signs of autoimmunity for a time period of 26 wk after virus infection. Uninfected WT and Siglec-H KO mice served as the control group. Just 8 wk after infection, significantly elevated ANA titers developed in Siglec-H KO mice, which increased gradually (Fig. 4 A, left). Infected WT control mice also showed a rise of ANAs, but delayed and significantly less than Siglec-H KO mice. Importantly, uninfected WT and Siglec-H KO control mice, which were observed for the same time period, did not develop ANAs (Fig. 4 A, right). Furthermore, infected Siglec-H KO mice generated elevated titers of anti-dsDNA IgG antibodies just 4 wk after infection that were significantly higher than anti-dsDNA titers of infected WT mice (Fig. 4 B, left). Again, anti-dsDNA antibodies were not detected in noninfected mice of the same age (Fig. 4 B, right). To screen for autoantibodies typical for SLE or related diseases, ELISAs for IgG autoantibodies against histones, nRNP (nuclear ribonucleoprotein), Sm (Smith antigen), SS-A (Sjörgen's syndrome–related antigen A; Ro), SS-B (Sjörgen's syndrome–related antigen B; La), and Scl-70 (scleroderma extractable immunoreactive fragment of 70 kD) were performed at the endpoint of the experiment, 26 wk after mCMV infection. Although no IgG antibodies were detected against SS-A, SS-B, or Scl-70, which are rare in SLE, or against nRNP, which is only found in a fraction of SLE patients (Rahman and Isenberg, 2008; unpublished data), antihistone and anti-Sm IgG were found in high levels only in infected Siglec-H KO mice but not in infected WT mice (Fig. 5).

The severity of glomerular nephritis can be determined by blood urea nitrogen (BUN) levels. BUN levels started to

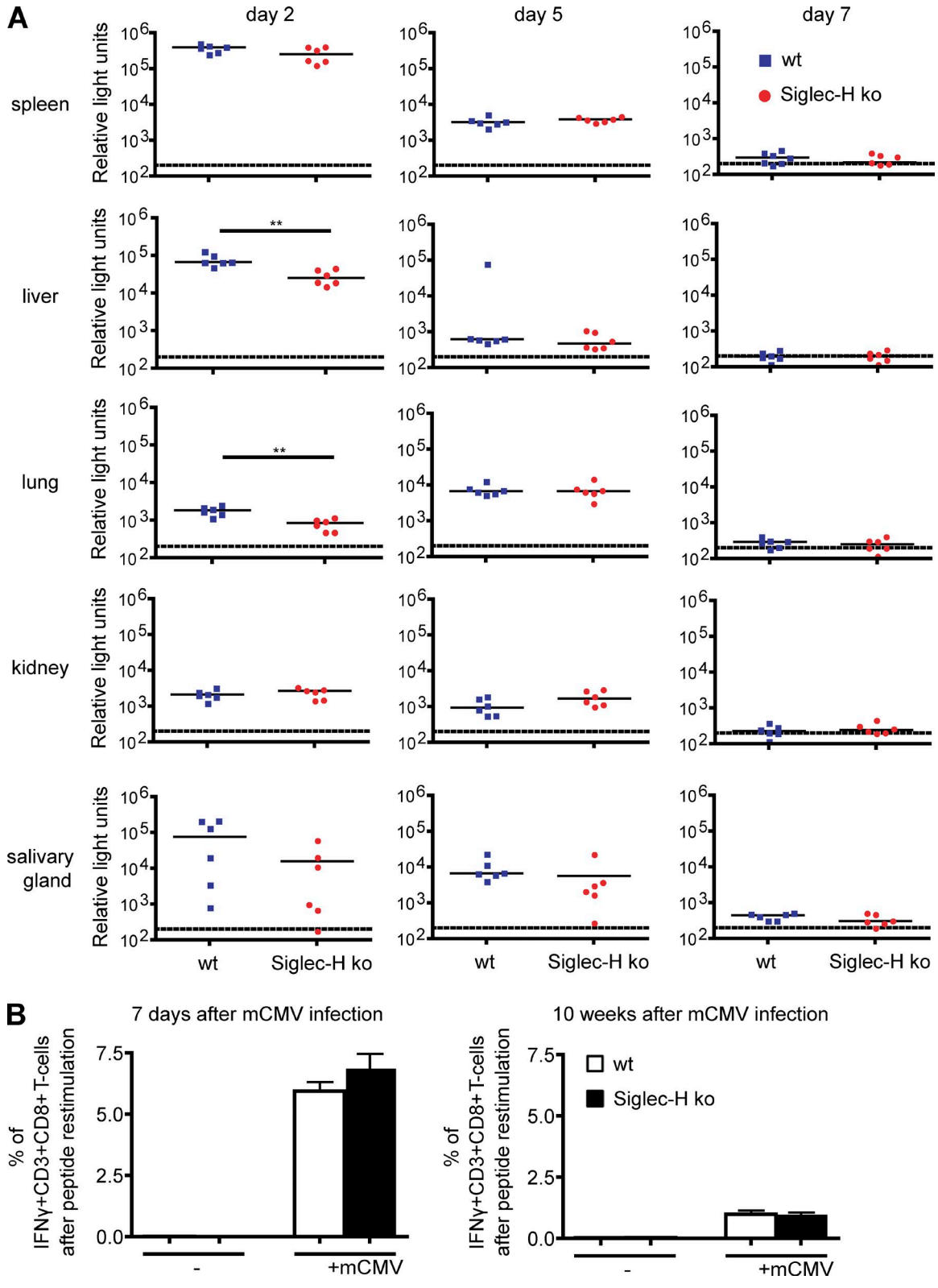

Figure 2. **Siglec-H KO mice show an overall normal virus control and no difference in the frequency of mCMV-specific CD8⁺ T lymphocytes.** (A and B) WT (wt) and Siglec-H KO (ko) mice were infected with 5×10^5 PFU MCMV157luc. (A) Different organs were collected after 2, 5, and 7 d to determine viral burden with a luciferase assay. Each symbol represents a single mouse. Median values are indicated by a line. Data are representative of three

rise in Siglec-H KO mice from 8 wk on after mCMV infection (Fig. 4 C, left). Infected WT mice also showed elevated BUN levels, but only to a moderate extent. At the end point (26 wk after infection), Siglec-H KO mice reached mean BUN levels of 72 mg/dl, almost the BUN level of 20–22-wk-old lupus MRL/*lpr* mice. In contrast, the mean BUN level of infected WT mice only reached 44 mg/dl (Fig. 4 C, left), whereas all uninfected WT and Siglec-H KO control mice had a normal range of 25–28 mg/dl.

Strong kidney damage and immune complex deposition in mCMV-infected Siglec-H KO mice

We next performed kidney histological studies to detect potential pathological alterations in the kidney morphology. Histopathological evaluation of kidneys from WT and Siglec-H KO mice 26 wk after mCMV infection revealed strong renal injury of infected Siglec-H KO mice typical for experimental lupus nephritis. Thus, we detected severe glomerular (Fig. 6, top), tubulointerstitial (Fig. 6, middle), and vascular (Fig. 6, bottom) alterations, including matrix expansion, abnormal glomerular basement membrane, thrombus formation, mesangial cell proliferation, and increased renal inflammation. These alterations were generally not found in WT infected mice or in uninfected mice at the same time point. In addition to renal alterations, we could detect IgG immune complex depositions in glomeruli of Siglec-H KO mice 26 wk after mCMV infection, which were significantly increased compared with infected WT mice (Fig. 7). Uninfected WT and Siglec-H KO control mice did not show any signs of immune complex deposition (Fig. 7). Hence, mCMV infection induces a severe lupus-like autoimmune disease with nephritis in Siglec-H KO mice.

No reactivation of mCMV virus but elevated type I IFN response genes 26 wk after mCMV infection in Siglec-H KO mice

Why do Siglec-H KO mice develop a severe autoimmune disease weeks after a single mCMV infection? First, we wanted to exclude that mCMV might be less efficiently controlled or is reactivated in Siglec-H KO mice at later time points after infection. After infection with CMV, the immune system controls replication, but the virus usually remains latent within the body throughout life and can be reactivated during periods of immunosuppression (Boeckh et al., 2003; Kotton et al., 2013; Lumbreras et al., 2014). To investigate whether reactivation of mCMV is involved in the severe lupus-like phenotype observed in infected Siglec-H KO mice, we measured the viral burden of WT and Siglec-H KO mice 10 and 26 wk after a single mCMV infection. We could not detect reactivation 10 wk (Fig. 8 A, left) or 26 wk (Fig. 8 A, right) after mCMV infection by luciferase assay in any organ. Furthermore, we performed a real-time PCR approach to detect mCMV DNA copies in different organs 26 wk after infection. In spleen and liver, mCMV DNA copy numbers were below or close to the detection limit (Fig. 8 B). In salivary gland and lung, very low DNA copy numbers in the range of 10–30 mCMV DNA copies/µg DNA were found. Importantly, mCMV copy numbers were not increased in infected Siglec-H KO mice (Fig. 8 B). Thus, we can exclude that virus reactivation plays a role in the observed lupus-like phenotype of infected Siglec-H KO mice. Because several studies have identified a type I IFN gene expression signature in most patients with active SLE (Baechler et al., 2003; Bennett et al., 2003), we assumed that an increased, uncontrolled type I IFN response in Siglec-H KO mice may trigger the development of autoimmune disease. Thus, we measured mRNA levels of typical type I IFN–inducible genes, namely *IRF7* and *CXCL10* (Baechler et al., 2003; Bennett et al., 2003), 10 and 26 wk after mCMV infection and in uninfected control mice. mCMV-infected Siglec-H KO mice showed a strong up-regulation of *IRF7* and *CXCL10* 10 and 26 wk (Fig. 9 A) after mCMV infection when compared with infected WT mice. At the end of the experiment (26 wk after mCMV infection), *IRF7* was 10-fold and *CXCL10* was 20-fold increased, showing a strong IFN signature in infected Siglec-H KO mice. No up-regulation of these two genes was observed in uninfected Siglec-H KO mice (Fig. 9 A). To get a more global view, gene array analysis was done of mCMV-infected or uninfected mice at the time point of 26 wk after infection. Fig. 9 B shows a hierarchical cluster analysis of 52 type I IFN–induced genes, chosen as described in the literature for induced genes in IFN-α–treated human PBMCs, which are to a large extent also up-regulated in human SLE patients (Baechler et al., 2003; Bennett et al., 2003). Almost one half (20/52) of type I IFN–inducible genes were significantly up-regulated in infected Siglec-H KO animals in comparison to infected WT, as well as in comparison to uninfected WT or to uninfected KO mice (Fig. 9 B).

mCMV-induced lupus-like phenotype of Siglec-H KO mice is type I IFN dependent

To prove whether the mechanism for the development of SLE-like autoimmunity triggered by mCMV is type I IFN dependent, we crossed WT and Siglec-H KO mice with IFN -α/β receptor (IFNAR) KO mice. The type I IFN receptor is broadly expressed on almost all cell types (Uzé et al., 2007), and we hypothesized that if the virus-induced autoimmunity depended on type I IFN, we would not observe

independent experiments ($n = 6$ for each experiment). **, $P < 0.01$. (B) 1.5×10^6 splenic cells/well (96-well plate, 200 µl of medium per well) were in vitro restimulated for 72 h with 0.75 µg/ml of a pool of mCMV-specific peptides (M33, M45, and M139) 7 d or 10 wk after mCMV infection. Intracellular IFN-γ production by $CD3^+CD8^+$ T cells was measured by flow cytometry. Data are representative of two independent experiments ($n = 6$ infected mice and $n = 3$ uninfected mice for each experiment). A Mann-Whitney test was used. Bar graphs show mean values with SEM.

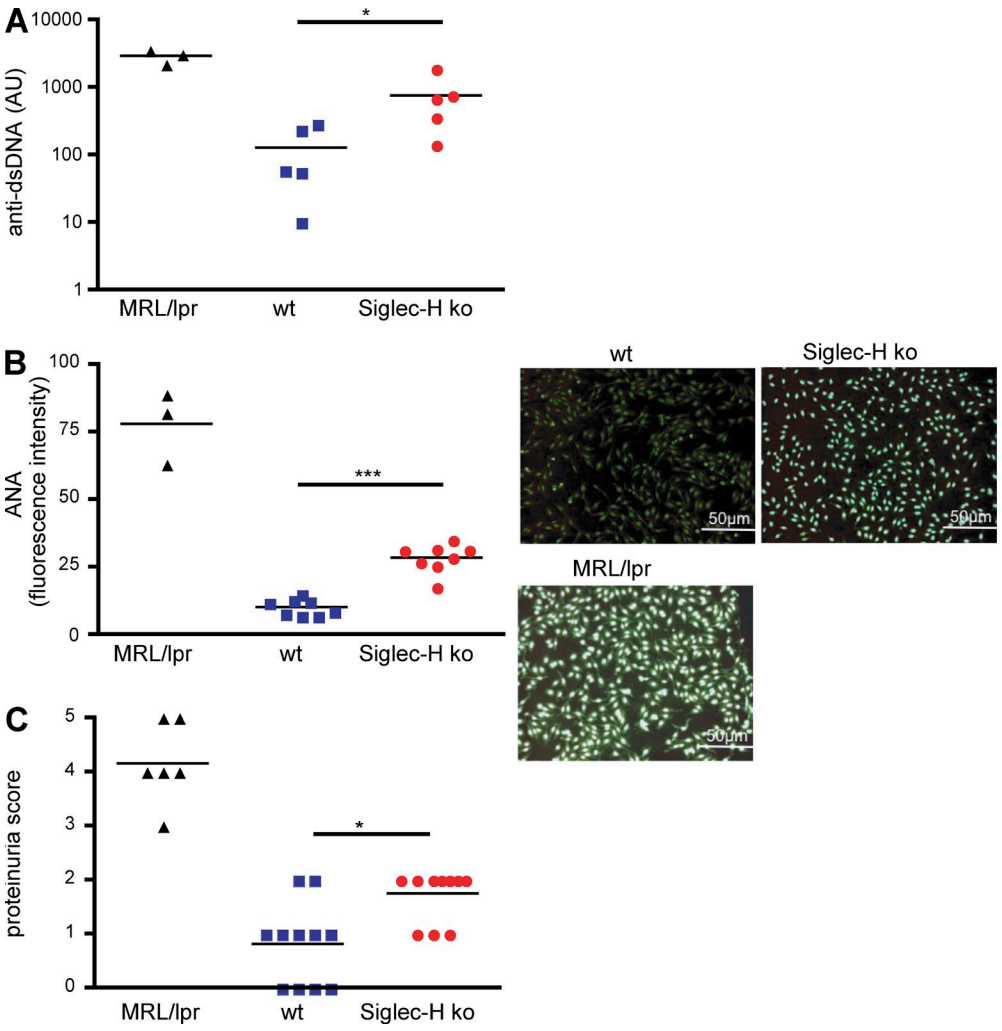

Figure 3. **Aging Siglec-H KO mice develop mild signs of autoimmunity.** (A) Anti-dsDNA in sera of 60-wk-old WT (wt) and Siglec-H KO (ko) mice was measured by ELISA. Each symbol represents a single mouse ($n = 5$ and $n = 3$ for MRL/*lpr* for each experiment). Data are representative of three independent experiments. AU, arbitrary units. (B) ANAs in sera of 60-wk-old WT and Siglec-H KO mice were semiquantitatively analyzed on HEp-2 slides. (Right) Example of fluorescent IgG autoantibodies in sera of WT, Siglec-H KO, and MRL/lpr mice on HEp-2 slides. (Left) The mean pixel intensity determined from 10 randomly analyzed cells in a sample is shown. Each symbol represents the IgG serum ANA level of a single mouse. The graph shows the summary of two independent experiments ($n = 8$ and $n = 3$ for MRL/*lpr*). (C) Proteinuria score of 60-wk-old WT and Siglec-H KO mice. The graph shows the summary of three independent experiments ($n = 10$–11 and $n = 6$ for MRL/*lpr*). *, $P < 0.05$; ***, $P < 0.001$; Mann-Whitney test. Sera of MRL/*lpr* mice served as a positive control.

this phenotype in IFNAR KO mice. We infected Siglec-H × IFNAR double KO, IFNAR KO, and as a control Siglec-H KO mice once with a lower dose of mCMV (10^4 PFU) to avoid lethality of acute mCMV infection in the absence of IFNAR signaling (Slavuljica et al., 2010). The typical signs of autoimmunity were recorded for a time period of 26 wk. In this experiment, we did not observe any autoimmunity development in IFNAR KO or Siglec-H × IFNAR double KO mice, whereas the control group of Siglec-H KO mice had ANAs, anti-dsDNA antibodies, and increased BUN levels starting after 8–12 wk (Fig. 10). This experiment clearly shows that the induction of autoimmune disease in Siglec-H KO mice by mCMV infection is strictly dependent on type I IFN signaling. In addition, this shows that a single low-level infection with 10^4 PFU mCMV was sufficient to induce autoimmune disease in the absence of Siglec-H.

DISCUSSION

In this study, we showed that Siglec-H prevents an mCMV-triggered autoimmunity in a type I IFN–dependent manner. The absence of Siglec-H resulted in a severe autoimmune disease in mCMV-infected Siglec-H KO mice. We demonstrated that virus-infected Siglec-H KO mice develop a type I IFN signature and also that Siglec-H–deficient pDCs produce higher IFN-α levels after TLR stimulation. One major function of pDCs is an initial defense against viruses by pro-

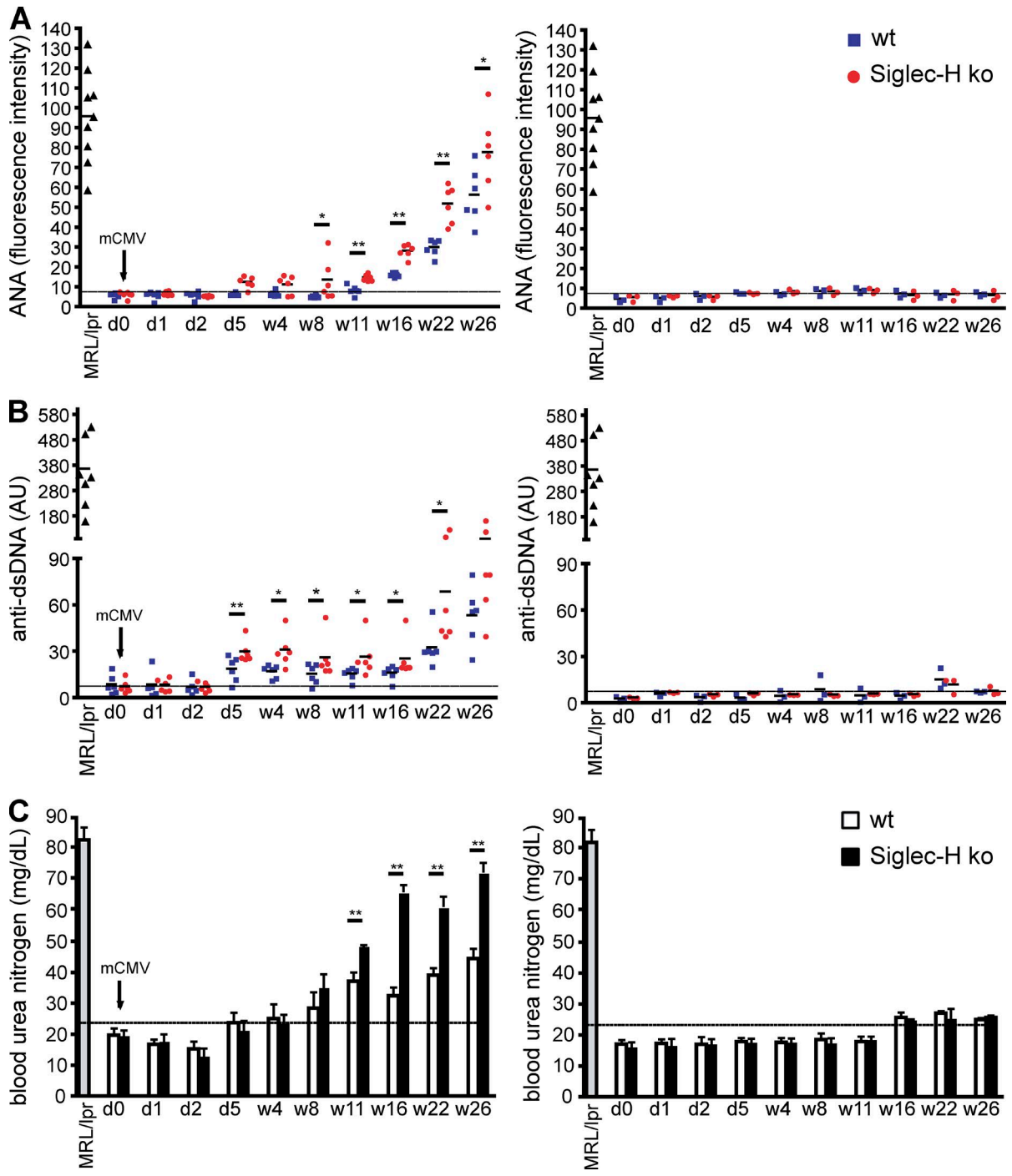

Figure 4. **mCMV-infected Siglec-H KO mice develop a severe lupus-like phenotype.** (A–C) WT (wt) and Siglec-H KO (ko) mice were once infected at day 0 with 5×10^5 PFU MCMV157luc, and typical signs of autoimmunity were monitored for a time period of 26 wk. Uninfected WT and Siglec-H KO mice served as the control group. (Left) mCMV-infected mice. (Right) Uninfected control mice. (A) ANAs in sera of mCMV-infected mice or uninfected control mice were semiquantitatively analyzed at different time points after infection on HEp-2 slides. The mean pixel intensity determined from 10 randomly analyzed cells in a sample is shown. Each symbol represents the IgG serum ANA level of a single mouse. (B) Anti-dsDNA in sera of mCMV-infected mice or uninfected control mice was measured by ELISA. Each symbol represents a single mouse. AU, arbitrary units. (C) Urea nitrogen contents in the blood of mCMV-infected mice or uninfected control mice were determined with an enzymatic BUN kit. The gray bars depict MRL/*lpr* mice. Data are representative of two independent experiments ($n = 6$ infected mice, $n = 3$ uninfected control mice, and $n = 5$–9 MRL/*lpr* mice for each experiment). *, $P < 0.05$; **, $P < 0.01$; Mann-Whitney test. Error bars are mean ± SEM values. Sera of MRL/*lpr* mice served as a positive control.

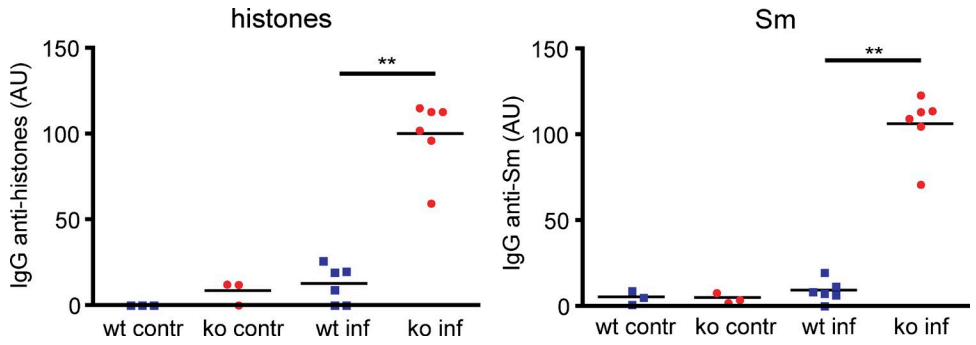

Figure 5. **mCMV-infected Siglec-H KO mice develop antihistone and anti-Sm autoantibodies with high prevalence.** IgG antihistone antibodies and anti-Sm antibodies were analyzed in sera obtained from mCMV-infected (inf) mice or uninfected control (contr) mice at week 26 after infection. Each symbol represents a single mouse. For a standard, a serum pool from diseased MRL/*lpr* mice was set to 200 arbitrary units (AU). **, $P < 0.01$; Mann-Whitney test. Data are representative of two independent experiments ($n = 6$ for infected mice and $n = 3$ for uninfected control mice for each experiment). ko, knockout; wt, wild type.

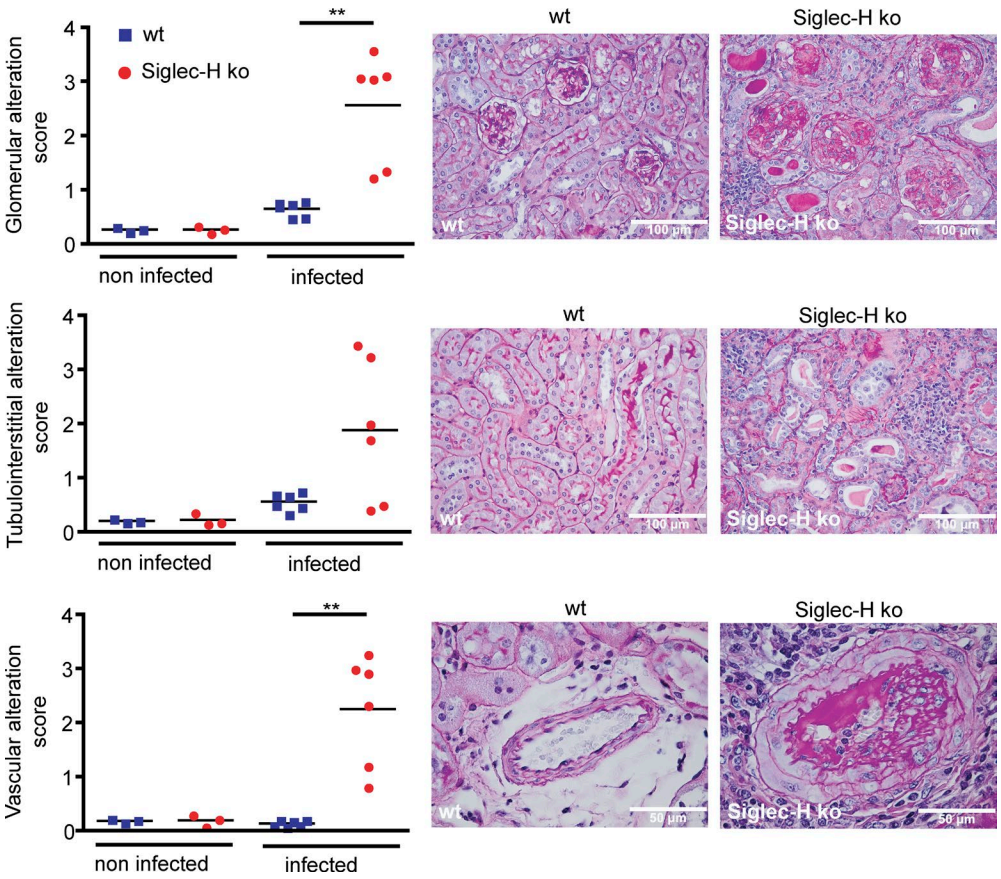

Figure 6. **mCMV-infected Siglec-H KO mice show strong kidney damage 26 wk after infection.** (Right) Shown are representative photomicrographs of periodic acid-Schiff–stained renal biopsies of infected WT (wt) and Siglec-H KO (ko) mice. Bars: (top and middle) 100 µm; (bottom) 50 µm. (Left) Kidneys from WT and Siglec-H KO mice were scored 26 wk after mCMV infection or for uninfected controls for typical changes observed in lupus nephritis. Severe glomerular (top), tubulointerstitial (middle), and vascular (bottom) alterations were observed in mCMV-infected Siglec-H KO mice. Each symbol represents a single mouse. Data are representative of two independent experiments ($n = 6$ for infected mice and $n = 3$ for uninfected controls for each experiment). **, $P < 0.01$; Mann-Whitney test.

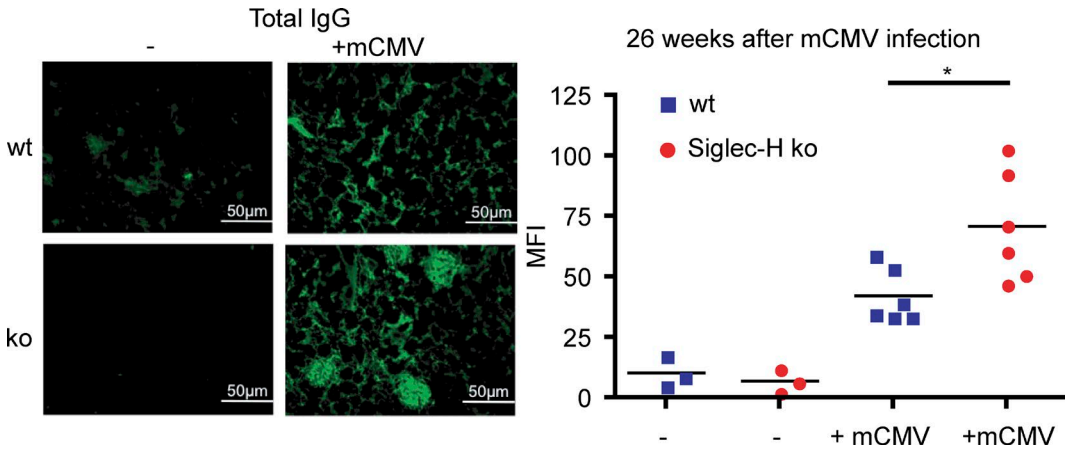

Figure 7. **Infected Siglec-H KO mice show increased immune complex depositions in the kidney 26 wk after mCMV infection.** (Left) WT (wt) and Siglec-H KO (ko) mice were infected once with 5×10^5 PFU MCMV157luc or left untreated, and immune complex depositions were analyzed on cryosections. Kidney sections were stained with fluorescence-conjugated antibodies against total IgG. Examples of stainings are shown for WT and Siglec-H KO mice, uninfected (–) or 26 wk after mCMV infection (+mCMV). (Right) Fluorescence intensity of immune complex depositions was quantified with ImageJ64. Each symbol represents the mean fluorescence intensity (MFI) of IgG depositions of a single kidney. Data are representative of two independent experiments ($n = 6$ infected mice and $n = 3$ uninfected mice for each experiment). *, $P < 0.05$; Mann-Whitney test.

ducing high type I IFN by TLR-dependent mechanisms. DNA viruses like CMV can enter pDCs via endocytosis and stimulate TLR9 in endosomes leading to IRF7-dependent stimulation of type I IFN genes (Swiecki and Colonna, 2015). Zhang et al. (2006) showed that Siglec-H can function as an endocytic receptor, but whether Siglec-H can capture and endocytose viruses or other pathogens for their delivery to TLR-containing endosomal compartments is unknown. Our results show that Siglec-H is not necessary for this function, as Siglec-H–deficient pDCs produce even more type I IFN in response to mCMV, and the infection rate of pDCs is not influenced by the loss of Siglec-H (Puttur et al., 2013). Even if Siglec-H is not directly involved in CMV internalization, Siglec-H might restrict the delivery of virus particles to the TLR9 endosomal compartment, thereby leading to modulated TLR9 stimulation.

Siglec-H itself does not contain signaling motifs in the cytoplasmic tail but can interact via its lysine residue in the transmembrane domain with the transmembrane adapter DAP12. DAP12 has two activatory immunoreceptor tyrosine-based activation motifs in its intracellular tail and can recruit Syk but paradoxically inhibits TLR-induced signaling in macrophages and pDCs (Sjölin et al., 2006; Turnbull and Colonna, 2007). DAP12-deficient pDCs lack Siglec-H surface expression and produce higher amounts of IFN-α and IL-12 after stimulation with CpG (Blasius and Colonna, 2006). Furthermore, DAP12-deficient macrophages secrete increased levels of proinflammatory cytokines, underlining the inhibitory role of DAP12 in these cells (Hamerman et al., 2005). DAP12 inhibits the response to TLR ligands through a so far unknown mechanism (Hamerman and Lanier, 2006), raising the possibility that the absence of Siglec-H impacts TLR signaling in a similar way as the absence of DAP12 does. It was shown that immunoreceptor tyrosine-based activation motif–coupled receptors in macrophages can inhibit type I IFN signaling and TLR signaling in a DAP12/Syk- and Pyk2-dependent way (Wang et al., 2010). Several other models have been discussed of how DAP12 might inhibit TLR signaling (Turnbull and Colonna, 2007), but further experiments are needed to study their potential role in the context of Siglec-H.

Most Siglecs recognize sialic acids in forms and linkages that are commonly found on cell surfaces and in the extracellular environment (Varki and Angata, 2006; Crocker et al., 2007). Although all necessary conserved amino acids for binding sialic acids are present within the N-terminal V-set Ig domain of Siglec-H, no binding to any sialic acids could so far be detected in a variety of attempts (Zhang et al., 2006). In contrast to other Siglecs, Siglec-H has two unpaired cysteines in domain 1 that could potentially form an intersheet disulfide bond. This might change the distance between the two β sheets, resulting in inhibition of sialic acid binding. These unusual cysteines can also be found in rat Siglec-H, which contain, in contrast to mouse Siglec-H, a serine instead of the conserved arginine in the N-terminal Ig domain (Zhang et al., 2006). It was hypothesized that Siglec-H might have evolved in rodents to act as a pattern recognition molecule, binding viral or other pathogen ligands similar to receptors of NK cells and myeloid cells (Arase et al., 2002; Zhang et al., 2006). So far, the natural ligand of Siglec-H still remains elusive.

Siglec-H was first described as a pDC-specific receptor (Blasius et al., 2006), but studies revealed that it is also expressed on a subset of marginal zone macrophages in the spleen, medullary macrophages in lymph nodes, and on microglia in the brain (Zhang et al., 2006; Kopatz et al., 2013). Because it was shown that MyD88 deficiency and depletion

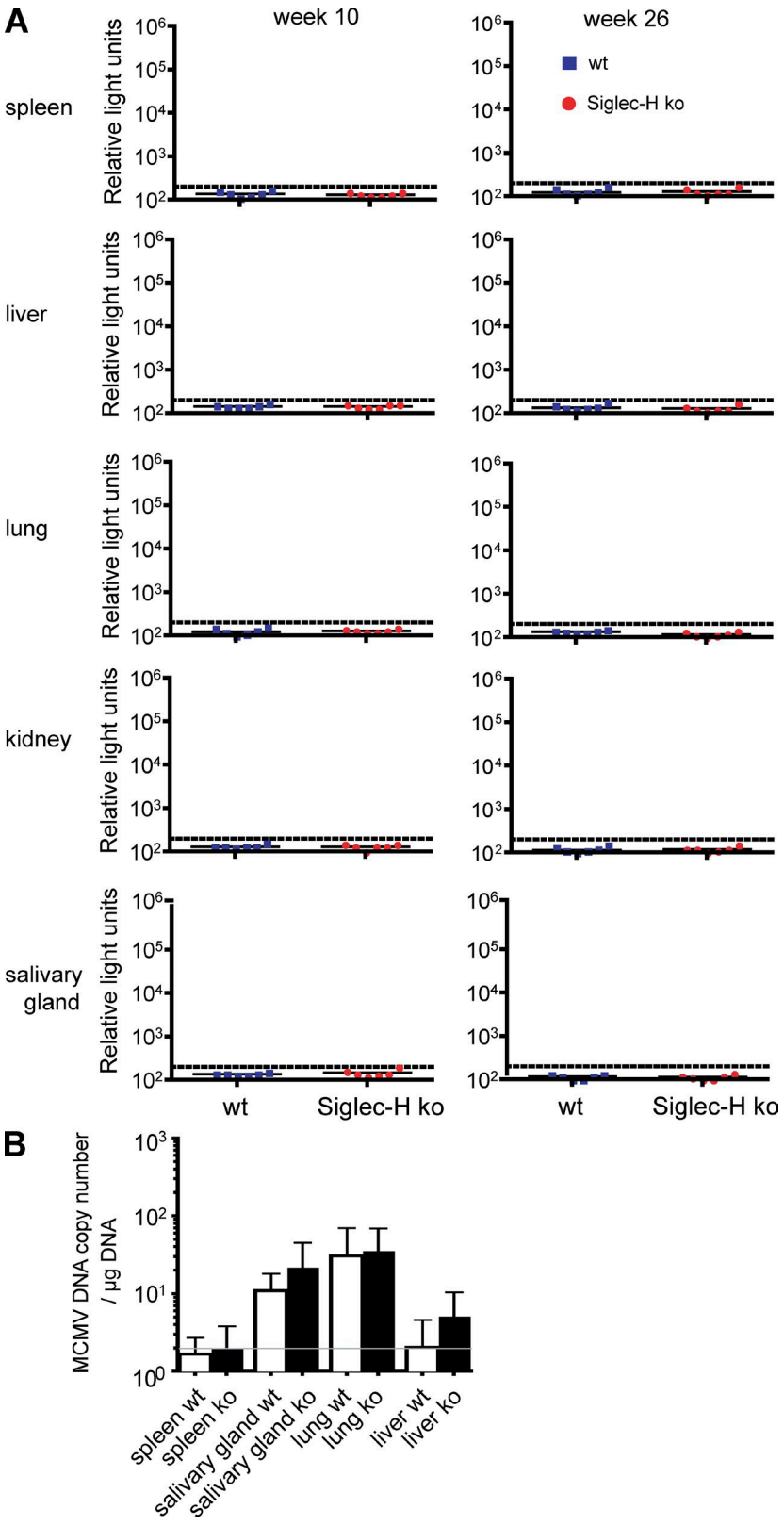

Figure 8. **No detectable virus reactivation 10 and 26 wk after mCMV infection.** (A and B) WT (wt) and Siglec-H KO (ko) mice were infected with 5×10^5 PFU MCMV157luc. (A) Different organs were collected after 10 and 26 wk to determine viral burden with a luciferase assay. Each symbol represents a single mouse. Data are representative of two independent experiments ($n = 6$ for each experiment). Medians are shown as dashed lines. (B) Viral DNA copies were determined by a real-time PCR assay from the indicated organs. The detection limit is indicated by the gray line. $n = 3$ each for WT and KO mice. The bar graph shows mean values with SEM.

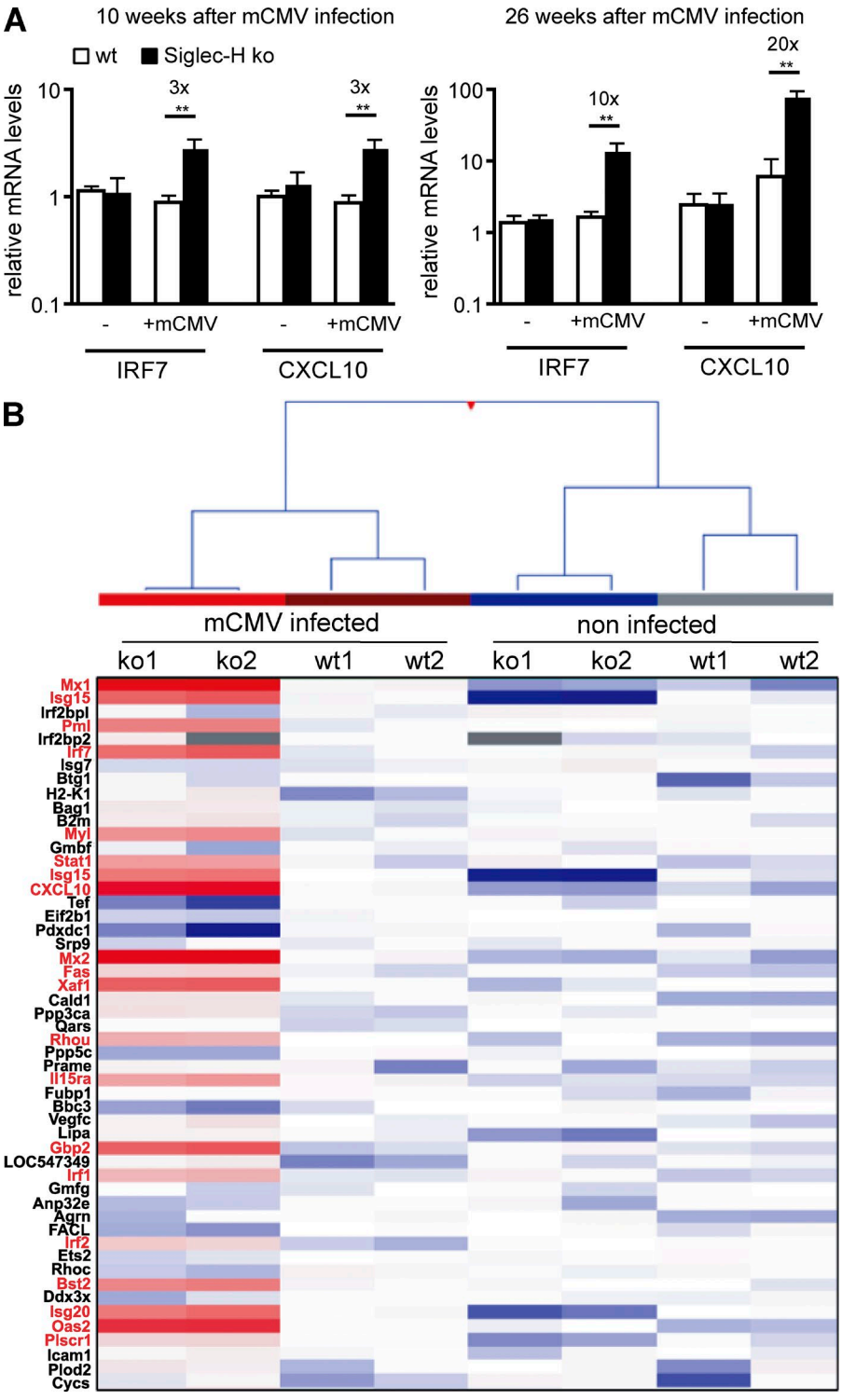

Figure 9. **mCMV-infected Siglec-H KO mice exhibit a strong up-regulation of type-I IFN response genes 26 wk after infection.** (A) RNA from splenic cells of mCMV-infected WT (wt) or Siglec-H KO (ko) mice and noninfected controls were isolated, and mRNA expression of different type I IFN–inducible genes was measured by qRT-PCR relative to mCMV-infected WT mice, whose expression levels were set to 1. Actin served as a housekeeping gene. Relative mRNA levels of *IRF7* and *CXCL10* 10 wk after mCMV infection and 26 wk after mCMV infection are shown. Data are representative of two independent experiments ($n = 6$ for each experiment). **, $P < 0.01$; Mann-Whitney test. Bar graphs show mean values with SEM. (B) Gene expression profiles of total splenic cells from two WT and Siglec-H KO mice 26 wk after mCMV infection and from two uninfected WT and Siglec-H KO control mice. Shown as a heat map are expression patterns of 52 type I IFN–inducible genes from microarray data, with the corresponding hierarchical clustering of the experimental conditions (mouse strain and infection status). Significantly up-regulated genes in infected Siglec-H KO mice in comparison to infected WT as well as to uninfected WT and to uninfected KO mice are marked in red (all red-marked genes are significantly up-regulated in all three conditions: KO infected vs. WT infected, KO uninfected, or WT uninfected). Pearson and Ward were used to compute hierarchical clustering of the experimental conditions (mouse strains and infection status). Expression data for each gene/row were normalized to the median expression value of the respective gene across all eight samples.

of pDCs early during an mCMV infection both do not substantially reduce type I IFN response gene expression (Cocita et al., 2015), it is likely that additional cell types other than pDCs are responsible for the type I IFN response. These other cell types may be Siglec-H–positive tissue macrophages that contribute to the protection from virus-induced autoimmunity. Two previous Siglec-H knock-in mice with disrupted Siglec-H reading frames led to controversial results regarding the contribution of Siglec-H on pDCs in type I IFN regulation. In one study, Siglec-H$^{DTR/DTR}$ mice were produced, and the resulting Siglec-H–deficient pDCs showed increased IFN-α levels after CpG stimulation in vitro (Tak-

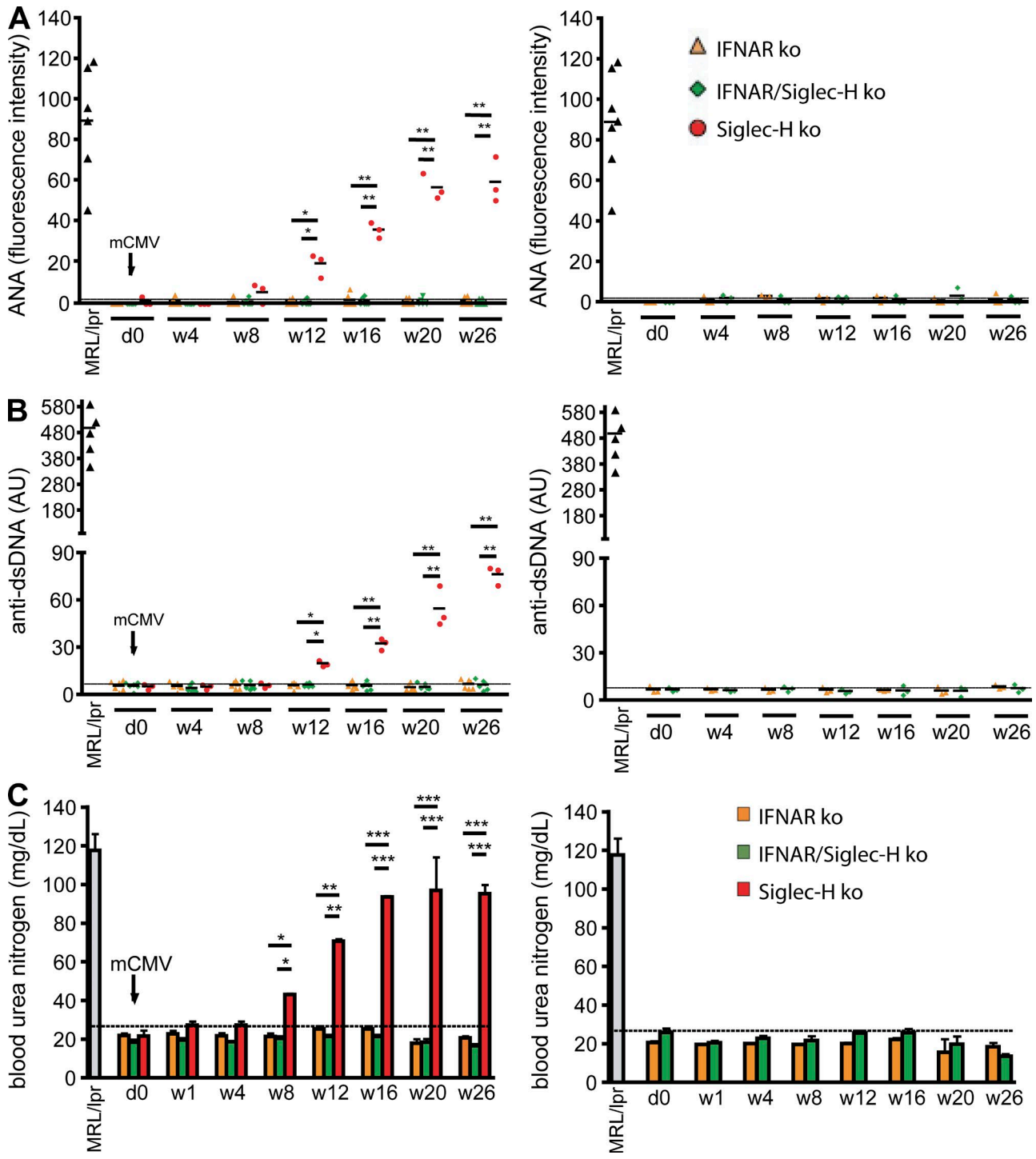

Figure 10. **mCMV-triggered autoimmune phenotype of Siglec-H KO mice is IFN-α dependent.** (A and B) IFNAR KO (ko), Siglec-H/IFNAR KO, and Siglec-H KO mice were once infected at day 0 with 10^4 PFU MCMV157luc, and typical signs of autoimmunity were monitored for a time period of 20 wk. Uninfected IFNAR KO and IFNAR/Siglec-H double KO mice served as the control group. (Left) mCMV-infected mice. (Right) Uninfected control mice. (A) ANAs in sera of mCMV-infected mice or uninfected control mice were semiquantitatively analyzed at different time points after infection on HEp-2 slides. The mean pixel intensity determined from 10 randomly analyzed cells in a sample is shown. Each symbol represents the IgG serum ANA level of a single mouse. (B) Anti-dsDNA in sera of mCMV-infected mice or uninfected control mice was measured by ELISA. Each symbol represents a single mouse. AU, arbitrary units. (C) Urea nitrogen contents in the blood of mCMV-infected mice or uninfected control mice were determined with an enzymatic BUN kit. The gray bars depict MRL/*lpr* mice. Bar graphs show mean values with SEM. Data are representative of two independent experiments (n = 6 infected mice and n = 3 uninfected mice for each experiment). *, $P < 0.05$; **, $P < 0.01$; ***, $P < 0.001$; Mann-Whitney test. Sera of MRL/*lpr* mice served as a positive control.

agi et al., 2011). Controversially, in another study, pDCs of Siglec-H$^{eGPF/eGPF}$ knock-in mice showed normal IFN-α responses after CpG or in vitro mCMV stimulation (Swiecki et al., 2014). These differences may be explained by different pDC preparation protocols. The latter Siglec-H–deficient mice showed enhanced IFN-α after HSV-1 infection, regardless of whether pDCs were depleted or not (Swiecki et al., 2014). The data from this mouse line suggest that other cell types like marginal zone macrophages or medullary macrophages are responsible for the enhanced type I IFN responses in vivo. Marginal zone macrophages were reported to be the main producers of type I IFN during HSV-1 infection (Eloranta and Alm, 1999). Therefore, the loss of Siglec-H on spleen or lymph node tissue macrophages in Siglec-H KO mice may contribute, in addition to pDCs, to the hyperproduction of type I IFN after mCMV infection.

We and others (Puttur et al., 2013; Swiecki et al., 2014) showed that the absence of Siglec-H resulted in an increase of IFN-α during the acute phase of mCMV infection. This elevated type I IFN response apparently triggers the development of a severe autoimmune disease in Siglec-H–deficient mice, as IFNAR KO mice did not show this phenotype. Siglec-H seems to be crucial to shut down type I IFN after persistent virus infections. Although we did not find an indication of higher viral DNA copies in Siglec-H KO mice several weeks after mCMV infection, we cannot exclude transient and promptly controlled events of virus reactivation occurring more frequently in the absence of Siglec-H. These events could constantly trigger low-level type I IFN responses. An inadequate control of type I IFN–inducible genes in infected Siglec-H KO mice could lead step by step to a hyperactivated milieu during the latent phase of mCMV infection, resulting in a severe lupus-like phenotype after 26 wk. Marshak-Rothstein (2006) proposed that virus-induced IFN-α initiates a self-perpetuating feedforward loop in which TLRs are up-regulated in B cells and cell death is promoted, which leads to increased release of intracellular autoantigens containing nucleic acids. The immune complexes formed with autoantibodies are internalized in pDCs and engage TLR7 or TLR9, which causes increased IFN-α production by pDCs (Marshak-Rothstein, 2006). As expected from this model, murine lupus–prone mouse strains, such as New Zealand mixed or *lpr* (Braun et al., 2003; Agrawal et al., 2009), showed a much milder lupus-like disease when crossed with IFNAR KO mice. In contrast, MRL/*lpr* mice unexpectedly showed a worse disease when crossed to IFNAR KO mice (Hron and Peng, 2004).

Despite one early observation of mild autoimmunity developing after mCMV infection in C57 Br/cdJ mice (Olding et al., 1976) and transient autoantibody productions against multiple organ-specific autoantigens, (Bartholomaeus et al., 1988) mCMV infections of laboratory mice have not been associated with any SLE-like disease so far. Our findings that antinuclear autoantibodies were developing over time to some extent in WT C57BL/6 mice are in line with these early observations. However, clinical signs for SLE-like autoimmunity were very mild in WT C57BL/6 mice previously infected with mCMV, in contrast to Siglec-H–deficient mice.

A correlation of CMV infection and development or exacerbation of SLE in humans has been discussed and is controversial (Halenius and Hengel, 2014). Also, infections with other persistent viruses like EBV and hepatitis C virus can lead to the production of transient ANAs in humans (McFarlane et al., 1995; Hansen et al., 1998; Harley and James, 2006). However, strong evidence for the link of virus infection to autoimmune disease is missing so far, mostly because of the lack of population-based prospective studies. One possible mechanism for the induction of autoimmunity by viral infection is molecular mimicry, when virus antigens share sequence or structural similarities with self-antigens (Oldstone, 1987). Because of the strong dependence of the CMV-induced autoimmune disease of Siglec-H–deficient mice on type I IFN, we consider molecular mimicry of CMV epitopes with self-antigens an unlikely explanation for our findings.

The severe autoimmune disease of Siglec-H–deficient mice was characterized by kidney pathology as indicated by severe glomerular, tubulointerstitial, and vascular changes, as well as by strongly increased BUN levels. This suggests that a certain threshold of type I IFN levels induced by virus infection is pathological and that this threshold is controlled by Siglec-H. So far, the impact of the loss of Siglec-H responses on the induction of autoimmune disease after virus infection has only been studied using mCMV. Also, the mCMV strain used here lacks the m157 protein and therefore escapes the efficient Ly49H$^+$ NK cell responses in C57BL/6 mice (Arase et al., 2002), which is, however, infrequently found in wild mice (Scalzo et al., 2005). In the future, it will be examined whether efficient antiviral NK cell responses might influence the autoimmune disease developing in Siglec-H KO mice upon mCMV infection. Furthermore, infections with other viruses will show whether these findings can be transferred to other viruses. It has been described that infection with another herpes virus, HSV-1, yielded to elevated IFN-α levels in Siglec-H mice as well (Takagi et al., 2011).

As CMVs extensively manipulate the innate as well as the adaptive immune system (Loewendorf and Benedict, 2010), the loss of self-tolerance and the induction of autoimmunity could be anticipated as a frequent event after infection. However, the long coevolution and cospeciation of CMVs with their hosts must have led to adaptation of the host and maybe also the virus to avoid clinical signs of autoimmunity (Halenius and Hengel, 2014). This appears particularly important for a pathogen that has a seroprevalence of 75–100% in natural wild populations, as described for mCMV (Smith et al., 1993; Goüy de Bellocq et al., 2015) as well as for human CMV (Cannon et al., 2011). It is evident that a critical balance of the innate and adaptive constituents of the immune system is necessary to provide sufficient power of the host defense mechanisms and at the same time to avoid loss of self-tolerance. Our studies described here sug-

gest that Siglec-H is part of such a delicate balance operating as a rheostat of type I IFN–driven autoimmunity after virus infection (Sharma et al., 2015).

Can these findings of Siglec-H KO mice be transferred to humans? Siglec-H is a mouse-specific Siglec and has no clear orthologue in humans (Crocker et al., 2007; Crocker and Redelinghuys, 2008). Nevertheless, there are other Siglecs that are mouse or human specific but share similar functions. For example, Siglec-8 on human eosinophils and mast cells and Siglec-F on murine eosinophils share similar expression patterns and are functionally related inhibitory receptors (Bochner, 2009). Even though Siglec-H has no clear orthologue in humans, there are potential functional homologues like the human Siglec-14 or Siglec-16. Both Siglecs are more broadly expressed on several myeloid cell types, but like Siglec-H, both interact with DAP12, which is crucial for their surface expression (Cao et al., 2008; Bochner, 2009). Interestingly, both the *SIGLEC-14* as well as the *SIGLEC-16* locus show widely spread polymorphisms in the human population. These polymorphic variants lead to the deletion of the DAP12-binding domain and replacement by another cytoplasmic Siglec domain (in the case of Siglec-14) or to a mutation of the coding region (in the case of Siglec-16), suggesting an ongoing evolution triggered by pathogens (Yamanaka et al., 2009; Wang et al., 2012). Furthermore, potential functional homologues to Siglec-H, which do not belong to the Siglec family, have been found on human pDCs. Both BDCA-2 and IL-T7 were shown to inhibit TLR-7/9–induced type I IFN production on human pDCs (Dzionek et al., 2001; Cao et al., 2006; Crozat et al., 2010).

To our knowledge, this is the first report of a surface receptor down-modulating immune responses to virus infection and thereby controlling autoimmunity. Because anti–Siglec-H antibodies have been shown to inhibit type I IFN production by pDCs (Blasius et al., 2004), this has a potential therapeutic application in the future.

MATERIALS AND METHODS

Mice. Siglec-H KO mice on a B6 background were obtained from the Consortium for Functional Glycomics by a gift from J. Paulson (Scripps Research Institute, La Jolla, CA). WT and Siglec-H KO mice were littermates of heterozygous breeding pairs. IFNAR KO mice were provided by U. Schleicher (University of Erlangen, Erlangen, Germany), originally a gift from U. Kalinke (Twincore, Hannover, Germany). Animal experiments were performed in accordance with the German law for protection of animals, after approval by the animal welfare committee (Regierung von Unterfranken).

mCMV strain and infection. The luciferase-encoding mCMV strain MCMV157luc was described previously (Klenovsek et al., 2007). To determine the virus titer by end-point titration, an indirect immunofluorescence on mouse embryonic fibroblasts was used as described previously (Klenovsek et al., 2007). Siglec-H mice were infected i.v. with 10^4 or 5×10^5 PFU of MCMV157luc. Measurement of virus titers in different organs (luciferase activity) was performed exactly as described previously (Klenovsek et al., 2007).

Detection of mCMV DNA by real-time PCR. Quantification of mCMV DNA copy numbers was performed on DNA isolated from the indicated organs by real-time PCR exactly as described by Klenovsek et al. (2007).

Generation of BM-derived pDCs. BM cells were isolated from femur and tibia. After red blood cell lysis with red blood cell lysis solution, BM cells from WT and Siglec-H KO mice were cultivated in complete RPMI (50 µM 2-mercaptoethanol, 1% nonessential amino acids, 1 mM sodium pyruvate, 100 µg/ml kanamycin sulfate, and 10% FCS [Sigma-Aldrich]) with 100 ng/ml rmFlt3L (R&D Systems) for 8 d at 2×10^6 cells/ml (25-cm^2 cell culture flasks, each with 5 ml of cells). After 4 d, 2.5 ml of medium per flask was replaced by 2.5 ml of fresh medium containing 50 ng/ml rmFlt3L. After 8 d, $CD11c^+PDCA^+$ pDCs were purified with magnetic-activated cell-sorting separation columns (Miltenyi Biotec).

In vitro stimulation of pDCs. pDCs were cultivated in 96-well plate (10^5 cells/well in 250 µl) using complete RPMI and were stimulated for 48 h with 2.5, 5, or 10 µg/ml CpG-A oligodeoxynucleotide 1585 (InvivoGen) or stimulated for 12, 24, or 48 h with MCMV157luc at a multiplicity of infection of 5.

Cytokine quantification. Supernatants from in vitro–stimulated pDCs or serum from mCMV mice were used to quantify cytokine concentrations by ELISA. To detect IFN-α by ELISA, MaxiSorp plates (Thermo Fisher Scientific) were coated with anti–mouse IFN-α (clone RMMA-1; Pestka Biomedical Laboratories [PBL] Interferon Source) and blocked with 1% BSA in PBS. 50 µl of samples/well was incubated overnight at 4°C. A polyclonal anti–IFN-α antibody from rabbit (PBL Interferon Source) and an HRP-conjugated anti–rabbit IgG (H+L) antibody (Dianova) served as secondary reagent. To measure HRP activity, OptEIA solution A/B (BD) was used and quantified at 570/450 nm. A mouse IFN-γ ELISA kit (Ready-SET-Go; Affymetrix; eBioscience) was used according to the manufacturer's instructions to detect IFN-γ levels by ELISA.

FACS analysis. Single-cell suspensions of BM, spleen, and lymph nodes were incubated with Gey's solution (for red blood cell lysis) to deplete erythrocytes. Staining was performed with the following antibodies (conjugated with FITC, PE, APC, and biotin): anti–Siglec-H (551.3D3; Miltenyi Biotec), anti-mPDCA1 (JF05-1C24.1; Miltenyi Biotec), anti-CD11c (N418; eBioscience), anti-B220 (RA3-6B2; eBioscience), and Fc-block (2.4G2; our hybridoma). Biotinylated antibodies were detected using streptavidin Cy5.5 (BD). Cells were analyzed using a flow cytometer (FACSCalibur; BD) and FlowJo software (Tree Star). Intracel-

lular staining after restimulation with mCMV-specific peptides was performed with a Cytofix/Cytoperm fixation/permeabilization solution kit (BD) according to the manufacturer's instructions.

Gene expression by quantitative RT-PCR (qRT-PCR). For qRT-PCR, RNA from 10^7 splenic cells was isolated by using QIAshredder and RNeasy kits (QIAGEN) according to the manufacturer's instructions. cDNA was synthesized using RNase H-Reverse transcription (Superscript III; Invitrogen), and qRT-PCR was performed on a quantitative PCR system (Stratagene Mx3000P) with green quantitative PCR Master Mix (Brilliant III Ultra-Fast SYBR; Agilent Technologies). mRNA expression of different type I IFN–inducible genes was measured by qRT-PCR relative to mCMV-infected WT mice, whose expression levels were set to 1. Actin served as the housekeeping gene. The following primers were used: actin forward, 5′-CCAACTGGGACGACATGGAG-3′; actin reverse, 5′-CTCGTAGATGGGCACAGTGTG-3′; CXCL10 forward, 5′-GCCGTCATTTTCTGCCTCATC-3′; CXCL10 reverse, 5′-CCAGTCATCGATATGGATGCA-3′; IRF7 forward, 5′-AAGGTGTACGAACTTAGCCG-3′; and IRF7 reverse, 5′-AAATGATCCGGACACACC-3′.

Microarray experiments. For microarray experiments, RNA from 10^7 splenic cells was isolated as described in the previous paragraph. RNA integrity was verified using a Nano Chip (RNA 6000; Agilent Technologies) on an BioAnalyzer (vB.02.03 BSI307; 2100; Agilent Technologies) as recommended by the manufacturer's protocol (RNA 6000 Nano Assay Protocol2). Sample labeling and preparation for microarray hybridization was essentially performed as described previously (Ferreira et al., 2010). The replicates of two Siglec-H KO or WT mice (mCMV infected or not infected) were hybridized onto a 4 × 44 K array (design-ID 026655; Agilent Technologies). Data were extracted with the feature extraction software package (v. 11.7.1; Agilent Technologies) using a standard protocol. The text files generated by the feature extraction software were imported into GeneSpring GX (v. 12.5; Silicon Genetics). Data were log2 transformed followed by normalization to the 75th percentile and corrected to the median of all samples. Features passing the quality check (flags detected in at least one condition) and showing changes in expression levels equal or more than twofold were selected for further analysis. A volcano plot was applied to identify statistically significant ($P > 0.05$), more than twofold differentially expressed genes between two conditions, including the Benjamini-Hochberg multiple test correction. Pearson and Ward were used to generate hierarchical clustering of the experimental conditions (mouse strains and infection status). Data were deposited in the GEO database under accession no. GSE79248.

Detection of ANAs on HEp-2 cells. ANAs were detected by incubating a 1:250 serum dilution on HEp-2 cells (Immco Diagnostics) according to the manufacturer's instructions. After 30-min incubation at room temperature, antinuclear total IgG was detected by Alexa Fluor 488–conjugated rabbit anti–mouse IgG (Invitrogen). Slides were analyzed with 10× magnification on a fluorescence microscope. ImageJ64 (National Institutes of Health) was used to determine the fluorescence intensity.

ELISA assays for antinuclear autoantibodies. Levels of anti-dsDNA were measured by ELISA. 0.01% poly-L-lysine (Sigma-Aldrich) was used to precoat MaxiSorp plates (Thermo Fisher Scientific). After 2 h at room temperature, plates were coated with dsDNA from 20 µg/ml calf thymus (Sigma-Aldrich) in H_2O overnight at 4°C. Plates were washed with PBS/0.05% Tween 20, and sera was added in 1:3 serial dilutions starting at 1:20; pooled serum of SLE-affected MRL/*lpr* mice, with a starting dilution of 1:250, served as the standard. 1 mg/ml goat anti–mouse IgG coupled to alkaline phosphatase was used for detection. A semiquantitative ELISA assay for IgG autoantibodies against histones, nRNP, Sm, SS-A (Ro), SS-B (La), and Scl-70 autoantibodies (Anti-ENA SLE-Profile 2; EUROIMMUN) and a quantitative ELI SA assay for IgG autoantibodies against Sm and histones were used as described by the manufacturer with the exception that an HRP-conjugated goat anti–mouse IgG antibody was used as the secondary antibody.

BUN. The enzymatic BUN kit from Stanbio Laboratory was used according to the manufacturer's instructions to examine the urea nitrogen content in blood. Therefore, sera were diluted 1:100 in enzymatic reagent on 96-well plates. After incubation in color reagent, urea nitrogen content was measured at a 600-nm wavelength with the ELISA reader (VersaMaxPLUS; Molecular Devices). Values <25 mg/dl were considered as normal.

Measurement of proteinuria. Fresh urine from mice was tested for protein with reagent strips for urine analysis (Albustix). Therefore, the color change of the strip was compared with a given color code with six different readings: negative (score 0), trace (score 1), 30 (score 2), 100 (score 3), 300 (score 4), and ≥2,000 (score 5) mg/dl protein.

Immunohistochemistry. Kidneys were harvested and snap frozen in optimal cutting temperature medium (TissueTEK; Sakura). 6-mm sections were fixed with ice-cold acetone on slides for 5 min after sectioning on a cryostat. Kidney sections were saturated with 20% horse serum in PBS for 1 h at room temperature and stained for immune complex depositions with anti-IgG–Alexa Fluor 488 (Invitrogen). After mounting with Mowiol mounting medium, slides were dried overnight at room temperature and analyzed on a fluorescence microscope. The microscope settings (exposure time, objective, illumination, and filter cube) were identical to allow comparison among samples within an experiment. ImageJ64 was used to determine the mean fluorescence intensity in the sections.

Histology. Kidneys were collected and fixed in 4% formalin overnight at room temperature, dehydrated, and embedded in paraffin. Sections, staining, and scoring were done as previously described (Bökers et al., 2014).

Statistics. Prism 4 (GraphPad Software) was used to calculate the statistics for all graphs shown. After testing for normal distribution, significant differences between samples were calculated using unpaired Student's *t* test or Mann-Whitney U-rank test. *, $P < 0.05$; **, $P < 0.01$; ***, $P < 0.001$.

Online supplemental material. Fig. S1 shows Siglec-H staining of pDCs of WT and Siglec-H KO mice and shows pDC numbers in three different organs of WT and Siglec-H KO mice. Online supplemental material is available at http://www.jem.org/cgi/content/full/jem.20160189/DC1.

ACKNOWLEDGMENTS

We thank the Consortium for Functional Glycomics for generating the Siglec-H KO mice and Dr. J. Paulson for providing them to us. We thank Dr. U. Kalinke for providing the IFNAR KO mice. We thank Stephen Reid and Andrea Schneider for technical help.

This work was funded by the Deutsche Forschungsgemeinschaft through grants GRK1660, TRR130, and CRC 1181 (project B06) to L. Nitschke and through grants GRK1660 and TRR130 to T.H. Winkler.

The authors declare no competing financial interests.

Submitted: 8 February 2016
Accepted: 13 May 2016

REFERENCES

Agrawal, H., N. Jacob, E. Carreras, S. Bajana, C. Putterman, S. Turner, B. Neas, A. Mathian, M.N. Koss, W. Stohl, et al. 2009. Deficiency of type I IFN receptor in lupus-prone New Zealand mixed 2328 mice decreases dendritic cell numbers and activation and protects from disease. *J. Immunol.* 183:6021–6029. http://dx.doi.org/10.4049/jimmunol.0803872

Arase, H., E.S. Mocarski, A.E. Campbell, A.B. Hill, and L.L. Lanier. 2002. Direct recognition of cytomegalovirus by activating and inhibitory NK cell receptors. *Science.* 296:1323–1326. http://dx.doi.org/10.1126/science.1070884

Baechler, E.C., F.M. Batliwalla, G. Karypis, P.M. Gaffney, W.A. Ortmann, K.J. Espe, K.B. Shark, W.J. Grande, K.M. Hughes, V. Kapur, et al. 2003. Interferon-inducible gene expression signature in peripheral blood cells of patients with severe lupus. *Proc. Natl. Acad. Sci. USA.* 100:2610–2615. http://dx.doi.org/10.1073/pnas.0337679100

Bartholomaeus, W.N., H. O'Donoghue, D. Foti, C.M. Lawson, G.R. Shellam, and W.D. Reed. 1988. Multiple autoantibodies following cytomegalovirus infection: virus distribution and specificity of autoantibodies. *Immunology.* 64:397–405.

Baumann, I., W. Kolowos, R.E. Voll, B. Manger, U. Gaipl, W.L. Neuhuber, T. Kirchner, J.R. Kalden, and M. Herrmann. 2002. Impaired uptake of apoptotic cells into tingible body macrophages in germinal centers of patients with systemic lupus erythematosus. *Arthritis Rheum.* 46:191–201. http://dx.doi.org/10.1002/1529-0131(200201)46:1<191::AID-ART10027>3.0.CO;2-K

Bennett, L., A.K. Palucka, E. Arce, V. Cantrell, J. Borvak, J. Banchereau, and V. Pascual. 2003. Interferon and granulopoiesis signatures in systemic lupus erythematosus blood. *J. Exp. Med.* 197:711–723. http://dx.doi.org/10.1084/jem.20021553

Blasius, A.L., and M. Colonna. 2006. Sampling and signaling in plasmacytoid dendritic cells: the potential roles of Siglec-H. *Trends Immunol.* 27:255–260. http://dx.doi.org/10.1016/j.it.2006.04.005

Blasius, A.L., W. Vermi, A. Krug, F. Facchetti, M. Cella, and M. Colonna. 2004. A cell-surface molecule selectively expressed on murine natural interferon-producing cells that blocks secretion of interferon-alpha. *Blood.* 103:4201–4206. http://dx.doi.org/10.1182/blood-2003-09-3108

Blasius, A.L., M. Cella, J. Maldonado, T. Takai, and M. Colonna. 2006. Siglec-H is an IPC-specific receptor that modulates type I IFN secretion through DAP12. *Blood.* 107:2474–2476. http://dx.doi.org/10.1182/blood-2005-09-3746

Bochner, B.S. 2009. Siglec-8 on human eosinophils and mast cells, and Siglec-F on murine eosinophils, are functionally related inhibitory receptors. *Clin. Exp. Allergy.* 39:317–324. http://dx.doi.org/10.1111/j.1365-2222.2008.03173.x

Boeckh, M., W.G. Nichols, G. Papanicolaou, R. Rubin, J.R. Wingard, and J. Zaia. 2003. Cytomegalovirus in hematopoietic stem cell transplant recipients: Current status, known challenges, and future strategies. *Biol. Blood Marrow Transplant.* 9:543–558. http://dx.doi.org/10.1016/S1083-8791(03)00287-8

Bogdanos, D.P., G. Mieli-Vergani, and D. Vergani. 2000. Virus, liver and autoimmunity. *Dig. Liver Dis.* 32:440–446. http://dx.doi.org/10.1016/S1590-8658(00)80266-2

Bökers, S., A. Urbat, C. Daniel, K. Amann, K.G. Smith, M. Espéli, and L. Nitschke. 2014. Siglec-G deficiency leads to more severe collagen-induced arthritis and earlier onset of lupus-like symptoms in MRL/lpr mice. *J. Immunol.* 192:2994–3002. http://dx.doi.org/10.4049/jimmunol.1303367

Braun, D., P. Geraldes, and J. Demengeot. 2003. Type I interferon controls the onset and severity of autoimmune manifestations in lpr mice. *J. Autoimmun.* 20:15–25. http://dx.doi.org/10.1016/S0896-8411(02)00109-9

Cannon, M.J., T.B. Hyde, and D.S. Schmid. 2011. Review of cytomegalovirus shedding in bodily fluids and relevance to congenital cytomegalovirus infection. *Rev. Med. Virol.* 21:240–255. http://dx.doi.org/10.1002/rmv.695

Cao, H., U. Lakner, B. de Bono, J.A. Traherne, J. Trowsdale, and A.D. Barrow. 2008. SIGLEC16 encodes a DAP12-associated receptor expressed in macrophages that evolved from its inhibitory counterpart SIGLEC11 and has functional and non-functional alleles in humans. *Eur. J. Immunol.* 38:2303–2315. http://dx.doi.org/10.1002/eji.200738078

Cao, W., D.B. Rosen, T. Ito, L. Bover, M. Bao, G. Watanabe, Z. Yao, L. Zhang, L.L. Lanier, and Y.J. Liu. 2006. Plasmacytoid dendritic cell-specific receptor ILT7-FcεRIγ inhibits Toll-like receptor-induced interferon production. *J. Exp. Med.* 203:1399–1405. http://dx.doi.org/10.1084/jem.20052454

Cervino, A.C., N.F. Tsinoremas, and R.W. Hoffman. 2007. A genome-wide study of lupus: preliminary analysis and data release. *Ann. N.Y. Acad. Sci.* 1110:131–139. http://dx.doi.org/10.1196/annals.1423.015

Cocita, C., R. Guiton, G. Bessou, L. Chasson, M. Boyron, K. Crozat, and M. Dalod. 2015. Natural killer cell sensing of infected cells compensates for MyD88 deficiency but not IFN-I activity in resistance to mouse cytomegalovirus. *PLoS Pathog.* 11:e1004897. http://dx.doi.org/10.1371/journal.ppat.1004897

Colonna, M., G. Trinchieri, and Y.J. Liu. 2004. Plasmacytoid dendritic cells in immunity. *Nat. Immunol.* 5:1219–1226. http://dx.doi.org/10.1038/ni1141

Crocker, P.R., and P. Redelinghuys. 2008. Siglecs as positive and negative regulators of the immune system. *Biochem. Soc. Trans.* 36:1467–1471. http://dx.doi.org/10.1042/BST0361467

Crocker, P.R., J.C. Paulson, and A. Varki. 2007. Siglecs and their roles in the immune system. *Nat. Rev. Immunol.* 7:255–266. http://dx.doi.org/10.1038/nri2056

Crozat, K., R. Guiton, M. Guilliams, S. Henri, T. Baranek, I. Schwartz-Cornil, B. Malissen, and M. Dalod. 2010. Comparative genomics as a tool to reveal functional equivalences between human and mouse dendritic cell subsets. *Immunol. Rev.* 234:177–198. http://dx.doi.org/10.1111/j.0105-2896.2009.00868.x

Dzionek, A., Y. Sohma, J. Nagafune, M. Cella, M. Colonna, F. Facchetti, G. Günther, I. Johnston, A. Lanzavecchia, T. Nagasaka, et al. 2001. BDCA-2, a novel plasmacytoid dendritic cell–specific type II C-type lectin, mediates antigen capture and is a potent inhibitor of interferon α/β induction. *J. Exp. Med.* 194:1823–1834. http://dx.doi.org/10.1084/jem.194.12.1823

Eloranta, M.L., and G.V. Alm. 1999. Splenic marginal metallophilic macrophages and marginal zone macrophages are the major interferon-α/β producers in mice upon intravenous challenge with herpes simplex virus. *Scand. J. Immunol.* 49:391–394. http://dx.doi.org/10.1046/j.1365-3083.1999.00514.x

Ferreira, S.J., M. Senning, S. Sonnewald, P.M. Kessling, R. Goldstein, and U. Sonnewald. 2010. Comparative transcriptome analysis coupled to X-ray CT reveals sucrose supply and growth velocity as major determinants of potato tuber starch biosynthesis. *BMC Genomics.* 11:93. http://dx.doi.org/10.1186/1471-2164-11-93

Goüy de Bellocq, J., S.J. Baird, J. Albrechtová, K. Sobeková, and J. Piálek. 2015. Murine cytomegalovirus is not restricted to the house mouse *Mus musculus domesticus*: prevalence and genetic diversity in the European house mouse hybrid zone. *J. Virol.* 89:406–414. http://dx.doi.org/10.1128/JVI.02466-14

Halenius, A., and H. Hengel. 2014. Human cytomegalovirus and autoimmune disease. *BioMed Res. Int.* 2014. http://dx.doi.org/10.1155/2014/472978

Hamerman, J.A., and L.L. Lanier. 2006. Inhibition of immune responses by ITAM-bearing receptors. *Sci. STKE.* 2006:re1.

Hamerman, J.A., N.K. Tchao, C.A. Lowell, and L.L. Lanier. 2005. Enhanced Toll-like receptor responses in the absence of signaling adaptor DAP12. *Nat. Immunol.* 6:579–586. http://dx.doi.org/10.1038/ni1204

Hansen, K.E., J. Arnason, and A.J. Bridges. 1998. Autoantibodies and common viral illnesses. *Semin. Arthritis Rheum.* 27:263–271. http://dx.doi.org/10.1016/S0049-0172(98)80047-4

Harley, J.B., and J.A. James. 2006. Epstein-Barr virus infection induces lupus autoimmunity. *Bull. NYU Hosp. Jt. Dis.* 64:45–50.

Harley, I.T., K.M. Kaufman, C.D. Langefeld, J.B. Harley, and J.A. Kelly. 2009. Genetic susceptibility to SLE: new insights from fine mapping and genome-wide association studies. *Nat. Rev. Genet.* 10:285–290. http://dx.doi.org/10.1038/nrg2571

Hooks, J.J., H.M. Moutsopoulos, S.A. Geis, N.I. Stahl, J.L. Decker, and A.L. Notkins. 1979. Immune interferon in the circulation of patients with autoimmune disease. *N. Engl. J. Med.* 301:5–8. http://dx.doi.org/10.1056/NEJM197907053010102

Hron, J.D., and S.L. Peng. 2004. Type I IFN protects against murine lupus. *J. Immunol.* 173:2134–2142. http://dx.doi.org/10.4049/jimmunol.173.3.2134

Jacobi, A.M., and B. Diamond. 2005. Balancing diversity and tolerance: lessons from patients with systemic lupus erythematosus. *J. Exp. Med.* 202:341–344. http://dx.doi.org/10.1084/jem.20050221

Klenovsek, K., F. Weisel, A. Schneider, U. Appelt, S. Jonjic, M. Messerle, B. Bradel-Tretheway, T.H. Winkler, and M. Mach. 2007. Protection from CMV infection in immunodeficient hosts by adoptive transfer of memory B cells. *Blood.* 110:3472–3479. http://dx.doi.org/10.1182/blood-2007-06-095414

Kopatz, J., C. Beutner, K. Welle, L.G. Bodea, J. Reinhardt, J. Claude, B. Linnartz-Gerlach, and H. Neumann. 2013. Siglec-h on activated microglia for recognition and engulfment of glioma cells. *Glia.* 61:1122–1133. http://dx.doi.org/10.1002/glia.22501

Kotton, C.N., D. Kumar, A.M. Caliendo, A. Asberg, S. Chou, L. Danziger-Isakov, and A. Humar. Transplantation Society International CMV Consensus Group. 2013. Updated international consensus guidelines on the management of cytomegalovirus in solid-organ transplantation. *Transplantation.* 96:333–360. http://dx.doi.org/10.1097/TP.0b013e31829df29d

Krug, A., A.R. French, W. Barchet, J.A. Fischer, A. Dzionek, J.T. Pingel, M.M. Orihuela, S. Akira, W.M. Yokoyama, and M. Colonna. 2004. TLR9-dependent recognition of MCMV by IPC and DC generates coordinated cytokine responses that activate antiviral NK cell function. *Immunity.* 21:107–119. http://dx.doi.org/10.1016/j.immuni.2004.06.007

Liu, Y.J. 2005. IPC: professional type 1 interferon-producing cells and plasmacytoid dendritic cell precursors. *Annu. Rev. Immunol.* 23:275–306. http://dx.doi.org/10.1146/annurev.immunol.23.021704.115633

Loewendorf, A., and C.A. Benedict. 2010. Modulation of host innate and adaptive immune defenses by cytomegalovirus: timing is everything. *J. Intern. Med.* 267:483–501. http://dx.doi.org/10.1111/j.1365-2796.2010.02220.x

Lumbreras, C., O. Manuel, O. Len, I.J. ten Berge, D. Sgarabotto, and H.H. Hirsch. 2014. Cytomegalovirus infection in solid organ transplant recipients. *Clin. Microbiol. Infect.* 20:19–26. http://dx.doi.org/10.1111/1469-0691.12594

Marshak-Rothstein, A. 2006. Toll-like receptors in systemic autoimmune disease. *Nat. Rev. Immunol.* 6:823–835. http://dx.doi.org/10.1038/nri1957

Marshak-Rothstein, A., and I.R. Rifkin. 2007. Immunologically active autoantigens: the role of toll-like receptors in the development of chronic inflammatory disease. *Annu. Rev. Immunol.* 25:419–441. http://dx.doi.org/10.1146/annurev.immunol.22.012703.104514

McFarlane, B.M., C.B. Bridger, H.M. Smith, K.A. Antonov, N. Naoumov, R. Williams, and I.G. McFarlane. 1995. Autoimmune mechanisms in chronic hepatitis B and delta virus infections. *Eur. J. Gastroenterol. Hepatol.* 7:615–621.

Moser, K.L., J.A. Kelly, C.J. Lessard, and J.B. Harley. 2009. Recent insights into the genetic basis of systemic lupus erythematosus. *Genes Immun.* 10:373–379. http://dx.doi.org/10.1038/gene.2009.39

Olding, L.B., D.T. Kingsbury, and M.B. Oldstone. 1976. Pathogenesis of cytomegalovirus infection. Distribution of viral products, immune complexes and autoimmunity during latent murine infection. *J. Gen. Virol.* 33:267–280. http://dx.doi.org/10.1099/0022-1317-33-2-267

Oldstone, M.B. 1987. Molecular mimicry and autoimmune disease. *Cell.* 50:819–820. http://dx.doi.org/10.1016/0092-8674(87)90507-1

Orr, S.L., D. Le, J.M. Long, P. Sobieszczuk, B. Ma, H. Tian, X. Fang, J.C. Paulson, J.D. Marth, and N. Varki. 2013. A phenotype survey of 36 mutant mouse strains with gene-targeted defects in glycosyltransferases or glycan-binding proteins. *Glycobiology.* 23:363–380. http://dx.doi.org/10.1093/glycob/cws150

Preble, O.T., R.J. Black, R.M. Friedman, J.H. Klippel, and J. Vilcek. 1982. Systemic lupus erythematosus: presence in human serum of an unusual acid-labile leukocyte interferon. *Science.* 216:429–431. http://dx.doi.org/10.1126/science.6176024

Puttur, F., C. Arnold-Schrauf, K. Lahl, G. Solmaz, M. Lindenberg, C. Mayer, M. Gohmert, M. Swalow, C. VanHelt, H. Schmitt, et al. 2013. Absence of Siglec-H in MCMV infection elevates interferon alpha production by plasmacytoid dendritic cells but does not enhance viral clearance. *PLoS Pathog.* http://dx.doi.org/10.1371/journal.ppat.1003648

Rahman, A., and D.A. Isenberg. 2008. Systemic lupus erythematosus. *N. Engl. J. Med.* 358:929–939. http://dx.doi.org/10.1056/NEJMra071297

Scalzo, A.A., M. Manzur, C.A. Forbes, M.G. Brown, and G.R. Shellam. 2005. NK gene complex haplotype variability and host resistance alleles to

murine cytomegalovirus in wild mouse populations. *Immunol. Cell Biol.* 83:144–149. http://dx.doi.org/10.1111/j.1440-1711.2005.01311.x

Schlitzer, A., V. Sivakamasundari, J. Chen, H.R. Sumatoh, J. Schreuder, J. Lum, B. Malleret, S. Zhang, A. Larbi, F. Zolezzi, et al. 2015. Identification of cDC1- and cDC2-committed DC progenitors reveals early lineage priming at the common DC progenitor stage in the bone marrow. *Nat. Immunol.* 16:718–728. http://dx.doi.org/10.1038/ni.3200

Sharma, S., K.A. Fitzgerald, M.P. Cancro, and A. Marshak-Rothstein. 2015. Nucleic acid–sensing receptors: Rheostats of autoimmunity and autoinflammation. *J. Immunol.* 195:3507–3512. http://dx.doi.org/10.4049/jimmunol.1500964

Sjölin, H., S.H. Robbins, G. Bessou, A. Hidmark, E. Tomasello, M. Johansson, H. Hall, F. Charifi, G.B. Karlsson Hedestam, C.A. Biron, et al. 2006. DAP12 signaling regulates plasmacytoid dendritic cell homeostasis and down-modulates their function during viral infection. *J. Immunol.* 177:2908–2916. http://dx.doi.org/10.4049/jimmunol.177.5.2908

Slavuljica, I., A. Busche, M. Babić, M. Mitrović, I. Gašparović, D. Cekinović, E. Markova Car, E. Pernjak Pugel, A. Ciković, V.J. Lisnić, et al. 2010. Recombinant mouse cytomegalovirus expressing a ligand for the NKG2D receptor is attenuated and has improved vaccine properties. *J. Clin. Invest.* 120:4532–4545.

Smith, A.L., G.R. Singleton, G.M. Hansen, and G. Shellam. 1993. A serologic survey for viruses and *Mycoplasma pulmonis* among wild house mice (*Mus domesticus*) in southeastern Australia. *J. Wildl. Dis.* 29:219–229. http://dx.doi.org/10.7589/0090-3558-29.2.219

Sundar, K., S. Jacques, P. Gottlieb, R. Villars, M.E. Benito, D.K. Taylor, and L.A. Spatz. 2004. Expression of the Epstein-Barr virus nuclear antigen-1 (EBNA-1) in the mouse can elicit the production of anti-dsDNA and anti-Sm antibodies. *J. Autoimmun.* 23:127–140. http://dx.doi.org/10.1016/j.jaut.2004.06.001

Swiecki, M., and M. Colonna. 2015. The multifaceted biology of plasmacytoid dendritic cells. *Nat. Rev. Immunol.* 15:471–485. http://dx.doi.org/10.1038/nri3865

Swiecki, M., S. Gilfillan, W. Vermi, Y. Wang, and M. Colonna. 2010. Plasmacytoid dendritic cell ablation impacts early interferon responses and antiviral NK and $CD8^+$ T cell accrual. *Immunity.* 33:955–966. http://dx.doi.org/10.1016/j.immuni.2010.11.020

Swiecki, M., Y. Wang, E. Riboldi, A.H. Kim, A. Dzutsev, S. Gilfillan, W. Vermi, C. Ruedl, G. Trinchieri, and M. Colonna. 2014. Cell depletion in mice that express diphtheria toxin receptor under the control of SiglecH encompasses more than plasmacytoid dendritic cells. *J. Immunol.* 192:4409–4416. http://dx.doi.org/10.4049/jimmunol.1303135

Takagi, H., T. Fukaya, K. Eizumi, Y. Sato, K. Sato, A. Shibazaki, H. Otsuka, A. Hijikata, T. Watanabe, O. Ohara, et al. 2011. Plasmacytoid dendritic cells are crucial for the initiation of inflammation and T cell immunity in vivo. *Immunity.* 35:958–971. http://dx.doi.org/10.1016/j.immuni.2011.10.014

Turnbull, I.R., and M. Colonna. 2007. Activating and inhibitory functions of DAP12. *Nat. Rev. Immunol.* 7:155–161. http://dx.doi.org/10.1038/nri2014

Uzé, G., G. Schreiber, J. Piehler, and S. Pellegrini. 2007. The receptor of the type I interferon family. *Curr. Top. Microbiol. Immunol.* 316:71–95.

Varki, A., and T. Angata. 2006. Siglecs—the major subfamily of I-type lectins. *Glycobiology.* 16:1R–27R. http://dx.doi.org/10.1093/glycob/cwj008

von Bernuth, H., C. Picard, A. Puel, and J.L. Casanova. 2012. Experimental and natural infections in MyD88- and IRAK-4-deficient mice and humans. *Eur. J. Immunol.* 42:3126–3135. http://dx.doi.org/10.1002/eji.201242683

Wang, L., R.A. Gordon, L. Huynh, X. Su, K.H. Park Min, J. Han, J.S. Arthur, G.D. Kalliolias, and L.B. Ivashkiv. 2010. Indirect inhibition of Toll-like receptor and type I interferon responses by ITAM-coupled receptors and integrins. *Immunity.* 32:518–530. http://dx.doi.org/10.1016/j.immuni.2010.03.014

Wang, X., N. Mitra, P. Cruz, L. Deng, N. Varki, T. Angata, E.D. Green, J. Mullikin, T. Hayakawa, and A. Varki. NISC Comparative Sequencing Program. 2012. Evolution of siglec-11 and siglec-16 genes in hominins. *Mol. Biol. Evol.* 29:2073–2086. http://dx.doi.org/10.1093/molbev/mss077

Yamanaka, M., Y. Kato, T. Angata, and H. Narimatsu. 2009. Deletion polymorphism of SIGLEC14 and its functional implications. *Glycobiology.* 19:841–846. http://dx.doi.org/10.1093/glycob/cwp052

Zhang, J.Q., B. Biedermann, L. Nitschke, and P.R. Crocker. 2004. The murine inhibitory receptor mSiglec-E is expressed broadly on cells of the innate immune system whereas mSiglec-F is restricted to eosinophils. *Eur. J. Immunol.* 34:1175–1184. http://dx.doi.org/10.1002/eji.200324723

Zhang, J.Q., A. Raper, N. Sugita, R. Hingorani, M. Salio, M.J. Palmowski, V. Cerundolo, and P.R. Crocker. 2006. Characterization of Siglec-H as a novel endocytic receptor expressed on murine plasmacytoid dendritic cell precursors. *Blood.* 107:3600–3608. http://dx.doi.org/10.1182/blood-2005-09-3842

Zucchini, N., G. Bessou, S.H. Robbins, L. Chasson, A. Raper, P.R. Crocker, and M. Dalod. 2008. Individual plasmacytoid dendritic cells are major contributors to the production of multiple innate cytokines in an organ-specific manner during viral infection. *Int. Immunol.* 20:45–56. http://dx.doi.org/10.1093/intimm/dxm119